Viable tensor-to-scalar ratio in a symmetric matter bounce

Rathul Nath Raveendran,[a] **Debika Chowdhury**[b] **and L. Sriramkumar**[b]

[a]The Institute of Mathematical Sciences, HBNI, CIT Campus, Chennai 600113, India
[b]Department of Physics, Indian Institute of Technology Madras, Chennai 600036, India

E-mail: rathulnr@imsc.res.in, debika@physics.iitm.ac.in, sriram@physics.iitm.ac.in

Abstract. Matter bounces refer to scenarios wherein the universe contracts at early times as in a matter dominated epoch until the scale factor reaches a minimum, after which it starts expanding. While such scenarios are known to lead to scale invariant spectra of primordial perturbations after the bounce, the challenge has been to construct *completely* symmetric bounces that lead to a tensor-to-scalar ratio which is small enough to be consistent with the recent cosmological data. In this work, we construct a model involving two scalar fields (a canonical field and a non-canonical ghost field) to drive the symmetric matter bounce and study the evolution of the scalar perturbations in the model. We find that the model can be completely described in terms of a single parameter, *viz.* the ratio of the scale associated with the bounce to the value of the scale factor at the bounce. We evolve the scalar perturbations numerically across the bounce and evaluate the scalar power spectra *after* the bounce. We show that, while the scalar and tensor perturbation spectra are scale invariant over scales of cosmological interest, the tensor-to-scalar ratio proves to be much smaller than the current upper bound from the observations of the cosmic microwave background anisotropies by the Planck mission. We also support our numerical analysis with analytical arguments.

Contents

1 Introduction

Bouncing models refer to scenarios wherein the universe undergoes a period of contraction until the scale factor attains a minimum value, whereupon it transits to the more standard phase of expansion. Such scenarios provide an alternative to the inflationary framework as they can also aid in overcoming the horizon problem associated with the conventional hot big bang model, in a fashion similar to inflation. Importantly, certain bouncing scenarios are also known to lead to nearly scale invariant spectra of primordial perturbations (see, for instance, the reviews [1–6]), as required by the cosmological data. It is generally expected that quantum gravitational effects will have a substantial influence on the dynamics of the very early universe, close to the big bang. In this work, we shall consider *classical bounces*,

which correspond to situations wherein the background energy density remains sufficiently lower than the Planckian energy density, even as the universe evolves across the bounce. This enables us to carry out our analysis without having to take into account possible Planck scale effects, which may otherwise play a significant role near the bounce.

Though there may be differences of opinion about the theoretical motivations for specific models, it has to be acknowledged that, as a broad paradigm, inflation has been a tremendous success (see, for example, the following reviews [7–15]). However, the remarkable effectiveness of the inflationary paradigm also seems to be responsible for its major drawback. Despite the strong observational constraints that have emerged, we still seem far from the desirable goal of arriving at a reasonably small subset of viable inflationary models (for a comprehensive list of single field models and their performance against the cosmological data, see Refs. [16–19]). Moreover, it is not clear whether the paradigm can be falsified at all (in this context, see Ref. [20])! In sharp contrast, bouncing models have been plagued by various difficulties and constructing a model that is free of pathologies, while being consistent with the observations, seems to pose considerable challenges. At this stage, we believe it is important that we highlight some of the generic issues. Firstly, in a universe which is undergoing accelerated expansion, any classical perturbations that are originally present in the sub-Hubble regime will quickly decay. But, such perturbations will rapidly grow during the contracting phase as one approaches the bounce. This behavior raises the concern if a smooth and homogeneous background that is required as an initial condition at suitably early times is sufficiently probable. It can also bring into question the validity of linear perturbation theory in the proximity of the bounce [3, 6, 21–23]. However, it has been shown that, for a large class of bouncing scenarios, one can work in a specific, well-defined gauge wherein linear perturbation theory is valid near the bounce (in this context, see Refs. [21, 22]). Secondly, small anisotropies are known to grow during the contracting phase, which may lead to the so-called Belinsky-Khalatnikov-Lifshitz instability [24]. While the above two issues can be alleviated to some extent in specific models such as the ekpyrotic scenario (see, for example, Refs. [25–28]), generically, they could be overcome only by careful fine tuning of the initial conditions (for a recent discussion on this point, see Ref. [29]). Thirdly, certain gauge invariant quantities are bound to diverge in the vicinity of the bounce [when the Null Energy Condition (NEC) is initially violated and later restored], which may pose fundamental difficulties in evolving the perturbations across the bounce. However, as we shall discuss in due course, this difficulty can be circumvented by working in a suitable gauge and evolving the perturbations in that particular gauge (in this context, see, for example, Ref. [30]). Fourthly, vector perturbations, if present, can grow rapidly in a contracting universe [22, 31]. But, this issue can be overcome if one assumes that there are no vector sources at early times. In spite of such issues, bouncing models have attracted a lot of attention in the literature over the last two decades (for an intrinsically incomplete list of efforts in this direction, see Refs. [25–57]). These efforts suggest that bouncing scenarios can be regarded as the most popular alternative to the inflationary paradigm. In this work, we shall consider a specific model leading to a completely symmetric matter bounce and investigate, both numerically and analytically, the evolution of scalar perturbations in this scenario.

A matter bounce corresponds to a certain class of bouncing scenarios wherein, during the early stages of the contracting phase, the scale factor behaves as in a matter dominated universe. Such models are known to be 'dual' to de Sitter inflation, and hence are expected to lead to scale invariant spectra of primordial perturbations [58, 59]. Before we go on to discuss about the specific model that we shall consider, let us make a few summarizing remarks

regarding the existing matter bounce models. One of the primary problems concerning symmetric matter bounce scenarios seems to be the fact that in many of these models [2, 3, 30, 42, 50], the tensor-to-scalar ratio r turns out to be far in excess of the current upper bound of $r \lesssim 0.07$ from the Planck mission [60]. One possible way of circumventing this difficulty seems to be to model the regular component as a perfect fluid. In particular, a suitably small speed of sound for the scalar perturbations ensures that the tensor-to-scalar ratio r is small enough to be consistent with the data [61, 62]. Due to the small speed of sound, the scalar perturbations leave the Hubble radius at earlier times (when compared with the tensor perturbations) providing them with more time for their amplitude to grow as the bounce is approached. It has been also been shown that, by making a judicious choice of the initial conditions, a small tensor-to-scalar ratio can be obtained in asymmetric bounces [30]. Within the context of Einsteinian gravity, it is well known that the NEC has to be violated in order to obtain a bounce. Moreover, since the Hubble parameter changes sign at the bounce, the total background energy density vanishes at the bounce. The simplest way to drive such a background would be to introduce a ghost field which carries a negative energy density (see, for instance, Refs. [30, 38, 40]). However, there are certain issues associated with ghost fields, mostly pertaining to the absence of a stable quantum vacuum [63]. The so-called ghost-condensate mechanism has been introduced as an improvement upon the typical ghost fields because the perturbative ghost instability can be avoided in this situation (see, for example, Refs. [43, 57]). Nevertheless, it has been shown that it is impossible to embed the ghost condensate Lagrangian into an ultraviolet complete theory [64]. In the matter bounce curvaton scenario [45], which also contains a ghost field in addition to a much lighter second field, the tensor-to-scalar ratio has been shown to be suppressed by 'kinetic amplification'. Another alternative would be to use the Galileon Lagrangian [44, 46, 56], wherein the gradient instability, which may otherwise lead to an exponential growth of the comoving curvature perturbation, can be avoided. In certain single field models which lead to a non-singular bounce, it has been argued that the scalar perturbations are amplified more during the bounce relative to the tensor perturbations, which may lead to a viable value of r [47, 53].

Therefore, the challenge seems to be to construct a *completely* symmetric matter bounce scenario wherein the tensor-to-scalar ratio is small enough to be in agreement with the observations. In an earlier work, we had studied the behavior of the tensor perturbations in a matter bounce scenario described by a specific form of the scale factor and had gone on to evaluate the tensor power spectrum and bispectrum in the model [65]. The most dominant of the primordial perturbations are, of course, the scalar perturbations. While the tensor perturbations are completely determined by the behavior of the scale factor, as is well known, the evolution of the scalar perturbations strongly depends on the nature of the source driving the background. In this work, assuming Einsteinian gravity, we shall construct a model that leads to the specific form of the scale factor for which we had previously obtained a scale invariant spectrum of tensor perturbations. As we shall see, the scale factor of our interest can be driven with the aid of two scalar fields, one of which is a canonical field described by a potential, whereas the other is a purely kinetic ghost field with a negative energy density. We shall show that it is possible to construct exact analytical solutions for the background dynamics of our model. Utilizing the analytical solutions for the background and, working in a specific gauge, we shall numerically evolve the perturbations across the bounce and evaluate the power spectrum of the scalar perturbations after the bounce. Interestingly, we find that the amplitude of the scale invariant scalar and tensor perturbation spectra

(over cosmological scales) are dependent on only one parameter, *viz.* the ratio of the scale associated with bounce to the value of scale factor at the bounce. Further, we shall illustrate that the tensor-to-scalar ratio is completely independent of even this parameter, and it is in agreement with the constraints from Planck. Lastly, we should mention that, we shall also present analytical arguments to support our numerical results.

This paper is organized as follows. In the following section, we shall quickly introduce the scale factor characterizing the bouncing scenario of our interest and stress a few basic points. In Sec. 3, to illustrate some aspects, we shall revisit the behavior of the tensor perturbations and the evaluation of the tensor power spectrum in the scenario. In Sec. 4, we shall construct the source for the bouncing scenario of our interest using two scalar fields. In Sec. 5, we shall first arrive at the equations of motion governing the scalar perturbations in a generic gauge. Thereafter, we shall obtain the reduced equations in a specific gauge wherein the perturbations behave well in the vicinity of the bounce. In Sec. 6, we shall evolve the scalar perturbations numerically across the bounce. In Sec. 7, we shall construct analytical solutions to the equations governing the perturbations under certain approximations and we shall show that the analytical arguments support our numerical results. In Sec. 8, we shall evaluate the scalar power spectrum and the tensor-to-scalar ratio after the bounce, both numerically as well as analytically, and illustrate that the resulting spectra are broadly in agreement with the constraints from the Planck data. We shall conclude in Sec. 9 with a summary and a brief outlook.

We shall work with natural units such that $\hbar = c = 1$, and set the Planck mass to be $M_{_{\rm Pl}} = (8\,\pi\,G)^{-1/2}$. We shall adopt the metric signature of $(-,+,+,+)$. Note that, while Greek indices shall denote the spacetime coordinates, the Latin indices shall represent the spatial coordinates, except for k which shall be reserved for denoting the wavenumber. Moreover, an overdot and an overprime shall denote differentiation with respect to the cosmic and the conformal time coordinates, respectively. We shall also work with a new time variable that we have introduced in an earlier work on bouncing scenarios, *viz.* e-$\mathcal{N}$-folds, which we denote as $\mathcal{N}$ [65, 66].

2 The scale factor describing the matter bounce

We shall consider the background to be the spatially flat, Friedmann-Lemaître-Robertson-Walker (FLRW) metric that is described by the line element

$$\mathrm{d}s^2 = -\mathrm{d}t^2 + a^2(t)\,\delta_{ij}\,\mathrm{d}x^i\,\mathrm{d}x^j = a^2(\eta)\,\left(-\mathrm{d}\eta^2 + \delta_{ij}\,\mathrm{d}x^i\,\mathrm{d}x^j\right), \tag{2.1}$$

where $a(t)$ is the scale factor and $\eta = \int \mathrm{d}t/a(t)$ denotes the conformal time coordinate. We shall assume that the scale factor describing the bounce is given in terms of the conformal time as follows:

$$a(\eta) = a_0\left(1 + \eta^2/\eta_0^2\right) = a_0\left(1 + k_0^2\,\eta^2\right), \tag{2.2}$$

where a_0 is the value of the scale factor at the bounce (*i.e.* at $\eta = 0$) and $k_0 = 1/\eta_0$ is the scale associated with the bounce. At very early times, *viz.* when $\eta \ll -\eta_0$, the scale factor behaves as $a \propto \eta^2$, which is the behavior in a matter dominated universe. It is for this reason that the above scale factor corresponds to a matter bounce scenario. In the absence of any other scale in the problem, it seems natural to assume that the quantity k_0 is related to the Planck scale. As we shall see later, the source driving the scale factor of our interest as well as the results we obtain depend only on the ratio k_0/a_0. Specifically, it is the dimensionless ratio

$k_0/(a_0\,M_{_{\rm Pl}})$ that shall determine the amplitude of the power spectra. We find that the scales of cosmological interest are about 20-30 orders of magnitude smaller than the wavenumber k_0 (in this context, see Ref. [65]).

Let us now highlight a few points concerning the above scale factor and the nature of the sources that are expected to drive the bounce. To begin with, the scale factor is completely symmetric about the bounce. Also, since the Hubble parameter $H = a'/a^2$ vanishes at the bounce, so does the total energy density, *i.e.* $\rho = 3\,H^2\,M_{_{\rm Pl}}^2$, of the sources driving the scale factor. It is straightforward to show that the energy density ρ too is symmetric about the bounce. The energy density initially increases on either side as one moves away from the bounce, reaches the maximum value $\rho_{\rm max} = 3^4\,M_{_{\rm Pl}}^2\,k_0^2/(4^3\,a_0^2)$ at $\eta = \pm\eta_*$, where $\eta_* = \eta_0/\sqrt{3}$, and decreases thereafter. Note that $\rho_{\rm max}$ depends only on the combination k_0/a_0. The fact that k_0/a_0 is the only parameter in the problem will become more evident when we attempt to model the sources that drive the bounce. If we assume $k_0/(a_0\,M_{_{\rm Pl}})$ to be, say, of the order of 10^{-5} or so, then, clearly, the energy density ρ will always remains much smaller than the Planckian density. It is for this reason that we are able to treat the bounce as completely classical. Interestingly, in the domain $-\eta_* < \eta < \eta_*$, wherein the energy decreases as one approaches bounce, one finds that $\dot{H} > 0$. Since $\dot{H} = -(\rho + p)/(2\,M_{_{\rm Pl}}^2)$, where p is the total pressure, $(\rho + p) < 0$ during this period. In other words, the NEC is violated over this domain. It should be clarified that, while $\eta_* \simeq 1/k_0$, the duration of the bounce in terms of the in terms of cosmic time is actually of the order of a_0/k_0.

It can be easily shown that the above scale factor can be driven by two fluids, one which is ordinary, pressureless matter and another which behaves exactly as radiation, albeit with a negative energy density [39, 67]. In fact, it is this negative energy density (and the associated negative pressure) that leads to the violation of the NEC near the bounce and also ensures that the total energy density of the two fluids vanishes at the bounce. In due course, we shall model these two fluids in terms of scalar fields.

3 The evolution of tensor perturbations and the tensor power spectrum

In this section, we shall revisit the evolution of the tensor perturbations and the evaluation of the corresponding power spectrum in the matter bounce scenario of our interest, which we have discussed in an earlier work [65]. We shall study the evolution of the perturbations analytically as well as numerically. This exercise permits us to introduce the concept of e-$\mathcal{N}$-folds and also highlight a few points concerning the evolution of perturbations in bouncing scenarios. Later, we shall adopt similar methods to obtain analytical solutions for the scalar perturbations. As we have emphasized earlier, the tensor perturbations are simpler to study because of the fact that the equation governing their evolution depends only on the scale factor.

3.1 Analytical evaluation of the tensor perturbations

Let us first discuss the analytical evaluation of the tensor modes and the tensor power spectrum.

When the tensor perturbations characterized by γ_{ij} are taken into account, the spatially flat FLRW metric can be expressed as (see, for instance, Refs. [7, 9–12])

$$\mathrm{d}s^2 = a^2(\eta)\,\left\{-\mathrm{d}\eta^2 + [\delta_{ij} + \gamma_{ij}(\eta, \boldsymbol{x})]\,\mathrm{d}x^i\,\mathrm{d}x^j\right\}. \tag{3.1}$$

The Fourier modes h_k corresponding to the tensor perturbations are governed by the differential equation

$$h_k'' + 2\,\frac{a'}{a}\,h_k' + k^2\,h_k = 0, \tag{3.2}$$

where, recall that, the overprimes denote differentiation with respect to the conformal time η. It proves to be convenient to introduce the so-called Mukhanov-Sasaki variable u_k defined through the relation: $h_k = \sqrt{2}\,u_k/(M_{_{\rm Pl}}\,a)$. The variable u_k satisfies the differential equation

$$u_k'' + \left(k^2 - \frac{a''}{a}\right)\,u_k = 0. \tag{3.3}$$

In the context of inflation, one imposes the standard Bunch-Davies initial condition on the modes when they are well inside the Hubble radius. As we shall soon discuss, in bouncing scenarios, such a condition can be imposed at sufficiently early times during the contracting phase. The tensor power spectrum, evaluated at a suitably late time, say, $\eta_{\rm e}$, is defined as

$$\mathcal{P}_{_{\rm T}}(k) = 4\,\frac{k^3}{2\,\pi^2}\,|h_k(\eta_{\rm e})|^2. \tag{3.4}$$

As is common knowledge, in the inflationary scenario, the power spectra are evaluated on super Hubble scales. In bouncing models, the spectra are typically evaluated some time after the bounce, when the universe is expected to make a transition to the conventional radiation dominated epoch.

From the expression (2.2) for the scale factor, we obtain that

$$\frac{a''}{a} = \frac{2\,k_0^2}{1 + k_0^2\,\eta^2}. \tag{3.5}$$

Clearly, the quantity a''/a exhibits a maximum at the bounce, with the maximum value being of the order of k_0^2, and it vanishes as $\eta \to \pm\infty$. For modes of cosmological interest such that $k \ll k_0$, we find that $k^2 \gg a''/a$ as $\eta \to -\infty$, *i.e.* at very early times. This behavior permits us to impose the standard Bunch-Davies initial condition on the modes u_k at early times.

As we mentioned, we shall be interested in evaluating the tensor power spectrum after the bounce. Let us assume that, after the bounce, the universe transits to the radiation domination epoch at, say, $\eta = \beta\,\eta_0$, where we shall set $\beta \simeq 10^2$. We should hasten to clarify that, while this value of β is somewhat arbitrary, we find that the final results do not strongly depend on the choice of β. In order to study the evolution of the tensor modes analytically, let us divide the period $-\infty < \eta \leq \beta\,\eta_0$ into two domains. The first domain is determined by the condition $-\infty < \eta \leq -\alpha\,\eta_0$, where α is a very large number, which we shall set to be 10^5. In other words, this domain corresponds to very early times during the contracting phase before the bounce. The second domain $-\alpha\,\eta_0 \leq \eta \leq \beta\,\eta_0$ evidently involves periods prior to as well as immediately after the bounce. We find that, under suitable approximations, we can evaluate the tensor modes analytically in both of these domains.

In the first domain (*i.e.* during $-\infty < \eta \leq -\alpha\,\eta_0$), the scale factor (2.2) reduces to

$$a(\eta) \simeq a_0\,k_0^2\,\eta^2, \tag{3.6}$$

so that we have $a''/a \simeq 2/\eta^2$, which is exactly the behavior in de Sitter inflation. The Bunch-Davies initial condition that are to be imposed on the mode u_k at early times when $k^2 \gg 2/\eta^2$ is given by [68]

$$u_k = \frac{1}{\sqrt{2\,k}}\,{\rm e}^{-i\,k\,\eta}. \tag{3.7}$$

The modes h_k that satisfy this initial condition in the first domain can be easily determined to be [58, 65, 69, 70]

$$h_k \simeq \frac{\sqrt{2}}{M_{_{\rm Pl}}}\,\frac{1}{\sqrt{2\,k}}\,\frac{1}{a_0\,k_0^2\,\eta^2}\,\left(1-\frac{i}{k\,\eta}\right)\,{\rm e}^{-i\,k\,\eta}. \tag{3.8}$$

Let us now consider the behavior of the modes in the second domain, *i.e.* $-\alpha\,\eta_0 \leq \eta \leq \beta\,\eta_0$. In this domain, for scales of cosmological interest, which correspond to $k \ll k_0$, the equation governing the tensor mode h_k simplifies to

$$h_k'' + \frac{2\,a'}{a}\,h_k' \simeq 0. \tag{3.9}$$

We should clarify that, since we are working in the domain wherein $\eta \geq -\alpha\,\eta_0$, this equation is actually valid for wavenumbers such that $k \ll k_0/\alpha$. The above equation can be integrated to yield

$$h_k(\eta) \simeq h_k(\eta_1) + h_k'(\eta_1)\,a^2(\eta_1)\,\int_{\eta_1}^{\eta}\frac{{\rm d}\tilde{\eta}}{a^2(\tilde{\eta})}, \tag{3.10}$$

where η_1 is a suitably chosen time, and we have set the constants of integration to be $h_k(\eta_1)$ and $h_k'(\eta_1)$. Upon choosing $\eta_1 = -\alpha\,\eta_0$ and using the form (2.2) of the scale factor, we find that, in the second domain, the tensor mode can be expressed as

$$h_k = \mathcal{A}_k + \mathcal{B}_k\,f(k_0\,\eta), \tag{3.11}$$

where

$$f(k_0\,\eta) = \frac{k_0\,\eta}{1+k_0^2\,\eta^2} + \tan^{-1}\,(k_0\,\eta)\,. \tag{3.12}$$

The quantities $\mathcal{A}_k$ and $\mathcal{B}_k$ can be determined from the solution (3.8) in the first domain and are given by

$$\mathcal{A}_k = \frac{\sqrt{2}}{M_{_{\rm Pl}}}\,\frac{1}{\sqrt{2\,k}}\,\frac{1}{a_0\,\alpha^2}\,\left(1+\frac{i\,k_0}{\alpha\,k}\right)\,{\rm e}^{i\,\alpha\,k/k_0} + \mathcal{B}_k\,f(\alpha), \tag{3.13a}$$

$$\mathcal{B}_k = \frac{\sqrt{2}}{M_{_{\rm Pl}}}\,\frac{1}{\sqrt{2\,k}}\,\frac{1}{2\,a_0\,\alpha^2}\,\left(1+\alpha^2\right)^2\,\left(\frac{3\,i\,k_0}{\alpha^2\,k}+\frac{3}{\alpha}-\frac{i\,k}{k_0}\right)\,{\rm e}^{i\,\alpha\,k/k_0}. \tag{3.13b}$$

It is interesting to note here that, after the bounce, the first term in $f(k_0\,\eta)$ decays while the second term exhibits a mild growth.

3.2 E-$\mathcal{N}$-folds and the numerical evaluation of the tensor modes

To understand the accuracy of the approximations involved, we can compare the above analytical results for the evolution of the tensor modes with the corresponding numerical results. Since the scale factor is specified, it is essentially a matter of numerically integrating the differential equation (3.2) governing the tensor perturbations with known coefficients. However, the conformal time coordinate does not prove to be an efficient time variable for numerical integration, in particular, when a large range in the scale factor needs to be covered. In the context of inflation, one works with e-folds N as the independent time variable, with the scale factor being given by $a(N) \propto {\rm e}^N$. But, the function ${\rm e}^N$ is monotonically increasing function, whereas, in a bounce, the scale factor decreases at first before beginning to increase.

In order to describe the completely symmetric bouncing universe of our interest, we shall introduce a new time variable $\mathcal{N}$, in terms of which the scale factor is given by [65, 66]

$$a(\mathcal{N}) = a_0\, \mathrm{e}^{\mathcal{N}^2/2}. \tag{3.14}$$

We shall refer to the variable $\mathcal{N}$ as e-$\mathcal{N}$-fold, and we shall perform the numerical integration using this variable. We shall assume that $\mathcal{N}$ is zero at the bounce, with negative values representing the phase prior to the bounce and positive values after.

In terms of e-$\mathcal{N}$-folds, the differential equation (3.2) governing the evolution of the tensor modes can be expressed as

$$\frac{\mathrm{d}^2 h_k}{\mathrm{d}\mathcal{N}^2} + \left(3\mathcal{N} + \frac{1}{H}\frac{\mathrm{d}H}{\mathrm{d}\mathcal{N}} - \frac{1}{\mathcal{N}}\right)\frac{\mathrm{d}h_k}{\mathrm{d}\mathcal{N}} + \left(\frac{k\,\mathcal{N}}{a\,H}\right)^2 h_k = 0, \tag{3.15}$$

where H is the Hubble parameter. In order to determine the coefficients of the above equation, we need to express the Hubble parameter in terms of e-$\mathcal{N}$-folds. Upon using the expression for the scale factor (2.2), we obtain that

$$\eta(\mathcal{N}) = \pm\, k_0^{-1}\, \left(\mathrm{e}^{\mathcal{N}^2/2} - 1\right)^{1/2}. \tag{3.16}$$

It is important to note that, since the Hubble parameter is negative during the contracting phase and positive during the expanding regime, we shall have to choose the root of $\eta(\mathcal{N})$ accordingly during each phase. We numerically integrate the differential equation (3.15) using a fifth order Runge-Kutta algorithm. We impose the initial conditions at a sufficiently early time, say, $\mathcal{N}_i$, when $k^2 = 10^4\,(a''/a)$. Evidently, the standard Bunch-Davies initial condition on u_k [cf. Eq. (3.7)] can be converted to initial conditions on the mode h_k and its derivative with respect to the e-$\mathcal{N}$-fold [65]. The tensor mode h_k evaluated numerically has been plotted in Fig. 1 for a specific wavenumber. In the same figure, we have also plotted the analytical result we have obtained for the tensor mode. It is clear from the figure that the analytical results match the exact numerical results exceedingly well, which illustrates the extent of accuracy of the analytical approximations.

3.3 Tensor power spectrum

The tensor power spectrum can now be evaluated using the solutions for the modes that we have obtained. Upon substituting the modes (3.11) in the expression (3.4), we find that the tensor power spectrum after the bounce, evaluated at $\eta = \beta\,\eta_0$, can be written as

$$\mathcal{P}_{_{\mathrm{T}}}(k) = 4\,\frac{k^3}{2\,\pi^2}\,|\mathcal{A}_k + \mathcal{B}_k\, f(\beta)|^2, \tag{3.17}$$

with $\mathcal{A}_k$ and $\mathcal{B}_k$ given by Eqs. (3.13), and f by Eq. (3.12). As we had pointed out, our approximations are valid only for modes such that $k \ll k_0/\alpha$. Also, for reasons discussed earlier, we need to choose β to be reasonably large. We have plotted the resulting tensor power spectrum in Fig. 2 for $k_0/(a_0\,M_{_{\mathrm{Pl}}}) = 3.3 \times 10^{-8}$, $\alpha = 10^5$ and $\beta = 10^2$. Clearly, the spectrum is scale invariant for wavenumbers such that $k \ll k_0/\alpha$. It is straightforward to determine the scale invariant amplitude of the power spectrum to be [58, 69, 70]

$$\mathcal{P}_{_{\mathrm{T}}}(k) \simeq \frac{9\,k_0^2}{2\,M_{_{\mathrm{Pl}}}^2\,a_0^2}. \tag{3.18}$$

Note that this tensor power spectrum depends only on the parameter k_0/a_0. As we shall illustrate later (see Fig. 6), the numerical results for the power spectrum (evaluated at $\eta = \beta\,\eta_0$) matches this scale invariant amplitude quite well.

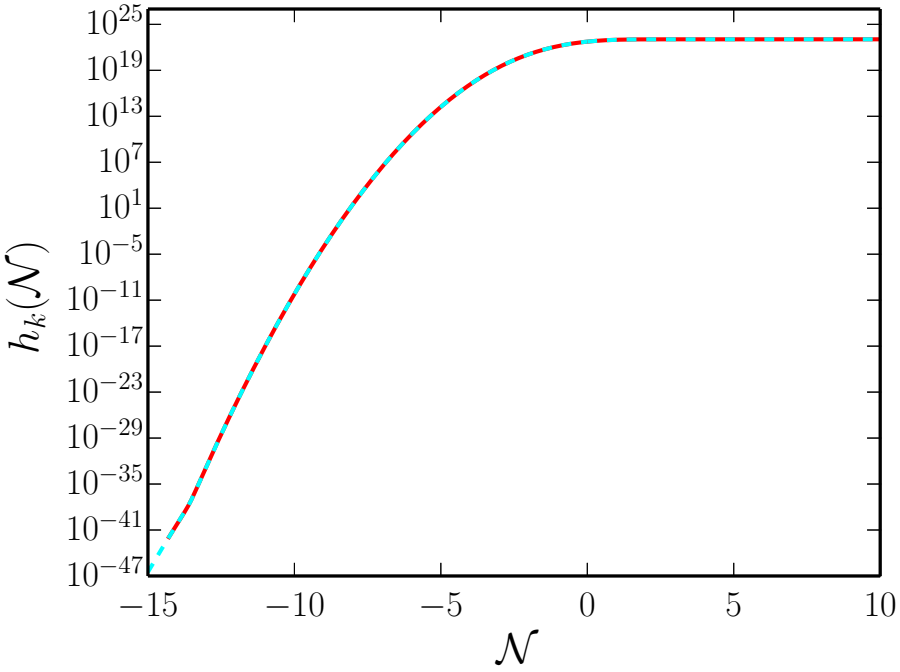

Figure 1. The numerical (in red) and the analytical (in cyan) results for the amplitude of the tensor mode h_k corresponding to the wavenumber $k/k_0 = 10^{-20}$ has been plotted as a function of e-$\mathcal{N}$-fold. We have set $k_0/(a_0\, M_{_{\rm Pl}}) = 3.3 \times 10^{-8}$ and, for plotting the analytical results, we have also chosen $\alpha = 10^5$. Note that, to arrive at the plots we have chosen $k_0 = M_{_{\rm Pl}}$ and $a_0 = 3.0 \times 10^7$, which is consistent with the abovementioned value of $k_0/(a_0\, M_{_{\rm Pl}})$. We have plotted the results from the initial e-$\mathcal{N}$-fold $\mathcal{N}_i$ [when $k^2 = 10^4\,(a''/a)$] corresponding to the mode. Clearly, the match between the analytical and numerical results is very good. This indicates that the approximation for determining the modes analytically works quite well.

4 Modeling the bounce with scalar fields

Our aim now is to construct sources involving scalar fields to drive the scale factor (2.2). We had mentioned earlier that the scale factor can be achieved with the aid of two fluids, one of which is pressureless matter and another which behaves as radiation, but with a negative energy density. It is well known that non-canonical scalar fields with a purely kinetic term can act as perfect fluids [71–75]. However, purely kinetic scalar fields cannot mimic pressureless matter, as a potential term is required to ensure that the pressure always remains zero. We shall model pressureless matter by a canonical scalar field with a potential, and describe radiation with negative energy density in terms of a suitable purely kinetic, non-canonical and ghost scalar field. As we had mentioned in the introductory section, such ghost fields pose certain conceptual difficulties. At this stage, we shall choose to overlook these difficulties and continue with our analysis. We shall make a few remarks about the issue in the concluding section.

Let the canonical field be ϕ and the non-canonical, ghost field be χ. We shall assume that the complete action describing these two fields is given by

$$S[\phi,\chi] = -\int {\rm d}^4x\,\sqrt{-g}\,\left[-X^{\phi\phi} + V(\phi) + U_0\,\left(X^{\chi\chi}\right)^2\right], \tag{4.1}$$

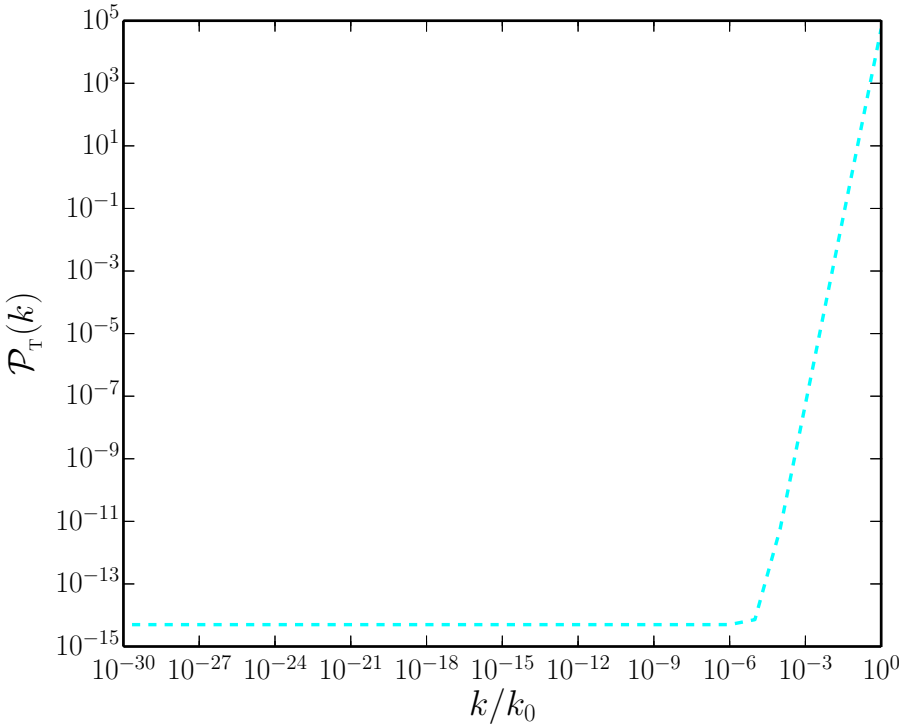

Figure 2. The tensor power spectrum $\mathcal{P}_{_{\rm T}}(k)$, evaluated analytically, has been plotted as a function of k/k_0 for a wide range of wavenumbers. In plotting this figure, we have chosen the same values for k_0/a_0 and α as in the previous figure, and have set $\beta = 10^2$. We should stress that the approximations we have worked with are valid only for wavenumbers such that $k \ll k_0/\alpha$. It is clear from the figure that the power spectrum is scale invariant over these wavenumbers. Note that, for the values of the parameters mentioned above, at small enough wavenumbers, the tensor power spectrum has the scale invariant amplitude of $\mathcal{P}_{_{\rm T}}(k) \simeq 5 \times 10^{-15}$.

where U_0 is a positive constant, and the kinetic terms $X^{\phi\phi}$ and $X^{\chi\chi}$ are defined as

$$X^{\phi\phi} = -\frac{1}{2}\,\partial_\mu\phi\,\partial^\mu\phi, \tag{4.2a}$$

$$X^{\chi\chi} = -\frac{1}{2}\,\partial_\mu\chi\,\partial^\mu\chi. \tag{4.2b}$$

The stress-energy tensor associated with these fields can be obtained to be

$$T^{\mu}_{\nu(\phi)} = \partial^\mu\phi\,\partial_\nu\phi - \delta^\mu_\nu\left[-X^{\phi\phi} + V(\phi)\right], \tag{4.3a}$$

$$T^{\mu}_{\nu(\chi)} = -2\,U_0\,X^{\chi\chi}\,\partial^\mu\chi\,\partial_\nu\chi - \delta^\mu_\nu\,U_0\,\left(X^{\chi\chi}\right)^2. \tag{4.3b}$$

Assuming the fields to be homogeneous, let us understand their behavior in a bouncing universe. Let us first consider the χ field. It is straightforward to obtain that

$$T^{0}_{0(\chi)} = -\rho_\chi = \frac{3\,U_0\,\dot{\chi}^4}{4}, \tag{4.4a}$$

$$T^{i}_{j(\chi)} = p_\chi\,\delta^i_j = -\frac{U_0\,\dot{\chi}^4}{4}\,\delta^i_j. \tag{4.4b}$$

Note that ρ_χ is negative and $p_\chi = \rho_\chi/3$, corresponding to radiation. In the absence of any potential, the equation of motion governing the field χ is extremely simple and is given by

$$\chi'' = 0. \tag{4.5}$$

This can be immediately integrated to obtain $\chi' = C_2$, where C_2 is a constant of integration. In other words, the field evolves monotonically towards either large or small values as the universe evolves. Such a behavior should not be surprising for a purely kinetic field that is devoid of any potential to guide it. The energy density ρ_χ can be written as

$$\rho_\chi = -\frac{3\,U_0\,\chi'^4}{4\,a^4} = -\frac{3\,U_0\,C_2^4}{4\,a^4}, \tag{4.6}$$

which is indeed the behavior of radiation, albeit with a negative energy density.

Let us now turn to the behavior of the field ϕ. The components of the stress-energy tensor associated with the field are given by

$$T^0_{0(\phi)} = -\rho_\phi = -\frac{\dot{\phi}^2}{2} - V(\phi), \tag{4.7a}$$

$$T^i_{j(\phi)} = p_\phi\,\delta^i_j = \left[\frac{\dot{\phi}^2}{2} - V(\phi)\right]\delta^i_j. \tag{4.7b}$$

Recall that the field ϕ is expected to behave as ordinary matter. The pressureless condition leads to [cf. Eq. (4.7b)]

$$\frac{\phi'^2}{2} - a^2\,V(\phi) = 0. \tag{4.8}$$

Further, being pressureless, the associated energy density is expected to behave as, say, $\rho_\phi = C_1^2/a^3$, where C_1 is a constant. This implies that we can can write [cf. Eq. (4.7)]

$$\frac{\phi'^2}{2} + a^2\,V(\phi) = \frac{C_1^2}{a}. \tag{4.9}$$

Upon adding the above two equations, we obtain that

$$\phi' = \frac{C_1}{\sqrt{a}}. \tag{4.10}$$

Given the scale factor (2.2), this equation can be easily integrated to arrive at

$$\phi = \phi_0\,\sinh^{-1}(k_0\,\eta), \tag{4.11}$$

where $\phi_0 = C_1/(\sqrt{a_0}\,k_0)$ and we have set the constant of integration to zero. The above expression can be inverted to write

$$k_0\,\eta = \sinh\left(\frac{\phi}{\phi_0}\right). \tag{4.12}$$

Since, according to Eqs. (4.8) and (4.10),

$$V(\phi) = \frac{\phi'^2}{2\,a^2} = \frac{C_1^2}{2\,a^3}, \tag{4.13}$$

on using the above solution for ϕ, we can determine the potential to be

$$V(\phi) = \frac{C_1^2}{2\,a_0^3\,\cosh^6\left(\phi/\phi_0\right)}. \tag{4.14}$$

It is straightforward to check that the above expressions for the field and the potential indeed satisfy the following standard equation of motion governing the canonical scalar field:

$$\ddot{\phi} + 3\,H\,\dot{\phi} + V_\phi = 0, \tag{4.15}$$

where $V_\phi = \mathrm{d}V/\mathrm{d}\phi$. Note that the evolution of the field is symmetric about the bounce. It starts with large negative values at early times during the contracting phase, rolls *up* the potential (4.14), reaching zero at the bounce[1]. Thereafter, the field continues towards positive values, rolling down the potential during the expanding phase.

Now that we have arrived at the behavior of the fields, the remaining task is to fix the constants C_1 and C_2. They ought to be related to the parameters a_0 and k_0 in terms of which we had expressed the scale factor and the constant U_0 that appears in the part of the action describing the field χ. We find that the first Friedmann equation $3\,H^2\,M_{_{\rm Pl}}^2 = \rho = \rho_\phi + \rho_\chi$ can be expressed as

$$3\,\mathcal{H}^2\,M_{_{\rm Pl}}^2 = \frac{\phi'^2}{2} + a^2\,V(\phi) - \frac{3\,U_0\,\chi'^4}{4\,a^2}, \tag{4.16}$$

where $\mathcal{H} = a'/a$ is the conformal Hubble parameter. Upon using the various expressions we have obtained above and the scale factor (2.2), we can determine the constants C_1 and C_2 to be

$$C_1 = \sqrt{12\,a_0}\,M_{_{\rm Pl}}\,k_0, \tag{4.17a}$$

$$C_2 = \sqrt{\frac{4\,M_{_{\rm Pl}}\,a_0\,k_0}{U_0^{1/2}}}, \tag{4.17b}$$

so that the energy densities associated with the two fields reduce to

$$\rho_\phi = \frac{12\,M_{_{\rm Pl}}^2\,a_0\,k_0^2}{a^3}, \tag{4.18a}$$

$$\rho_\chi = -\frac{12\,M_{_{\rm Pl}}^2\,a_0^2\,k_0^2}{a^4}. \tag{4.18b}$$

It is easy to see that $\rho_\phi + \rho_\chi = 0$ at the bounce, and such a behavior would not have been possible without the ghost field χ.

We should point out here that, if we make use the above expression for C_1, the potential (4.14) can be written as

$$V(\phi) = \frac{6\,M_{_{\rm Pl}}^2\,(k_0/a_0)^2}{\cosh^6\left(\sqrt{12}\,\phi/M_{_{\rm Pl}}\right)}. \tag{4.19}$$

[1]The fact that the field rolls *up* the potential during the contracting phase should not come as a surprise. During an expanding phase such as inflation, H is positive and, as is well known, the $3\,H\,\dot{\phi}$ term leads to friction, slowing down the field that is rolling down a potential. In contrast, during a contracting phase, since H is negative, the $3\,H\,\dot{\phi}$ term acts as 'anti-friction', speeding up the field and thereby allowing it to climb the potential.

In other words, the potential and, hence, the complete model, actually depends *only* on the parameter k_0/a_0. Therefore, we can expect the power spectra to depend only on this combination. This is already evident in the case of the tensors [cf. Eq. (3.18)]. In due course, we shall see that similar conclusions apply to the scalars as well. We shall comment further on this point in the concluding section.

We should mention here that the matter bounce scenario driven by two scalar fields we are studying is somewhat similar to a system which had been investigated earlier [30]. In the earlier work, the purely kinetic, ghost field χ was described by a linear kinetic term, in contrast to the non-linear term that we are considering. Also, the choice of the potential describing the canonical field ϕ was different. However, since both the models lead to a matter dominated phase at early times, we find that the two potentials behave in a similar manner at large negative values of the field. The difference in the action governing the χ field and the choice of an even function for the potential describing the ϕ field lead to a difference in the behavior of the background around the bounce between the two models. Our choices not only permit us to solve for the background analytically, but, importantly, the symmetric matter bounce (2.2) of our interest leads to a tensor-to-scalar ratio that is consistent with the observations.

5 Equations of motion governing the scalar perturbations

In this section, we shall derive the equations governing the evolution of the scalar perturbations. Since there are two fields involved, evidently, apart from the curvature perturbation, there will be an isocurvature perturbation present as well. We shall derive the equations governing the perturbations $\delta\phi$ and $\delta\chi$ and their corresponding gauge invariant versions $\overline{\delta\phi}$ and $\overline{\delta\chi}$. Thereafter, we shall construct the curvature and isocurvature perturbations for our model and arrive at the corresponding equations governing them.

5.1 The first order Einstein's equations

If we take into account the scalar perturbations to the background metric, then the FLRW line-element, in general, can be written as (see, for instance, Refs. [7, 9–12])

$$\mathrm{d}s^2 = -\left(1+2\,A\right)\,\mathrm{d}t^2 + 2\,a(t)\,\left(\partial_i B\right)\,\mathrm{d}t\,\mathrm{d}x^i + a^2(t)\,\left[\left(1-2\,\psi\right)\,\delta_{ij} + 2\,\left(\partial_i\,\partial_j E\right)\right]\,\mathrm{d}x^i\,\mathrm{d}x^j, \tag{5.1}$$

where A, B, ψ and E are four scalar functions that describe the perturbations, which depend on time as well as space. At the first order in the perturbations, the Einstein's equations are given by [7, 9–12]

$$3\,H\,\left(H\,A+\dot{\psi}\right) - \frac{1}{a^2}\,\nabla^2\left[\psi - a\,H\,\left(B-a\,\dot{E}\right)\right] = -\frac{1}{2\,M_{_{\rm Pl}}^2}\,\left(\delta\rho_\phi+\delta\rho_\chi\right), \tag{5.2a}$$

$$\partial_i\left(H\,A+\dot{\psi}\right) = \frac{1}{2\,M_{_{\rm Pl}}^2}\,\partial_i\left(\delta q_\phi+\delta q_\chi\right), \tag{5.2b}$$

$$\ddot{\psi} + H\,\left(\dot{A}+3\,\dot{\psi}\right) + \left(2\,\dot{H}+3\,H^2\right)\,A = \frac{1}{2\,M_{_{\rm Pl}}^2}\,\left(\delta p_\phi+\delta p_\chi\right), \tag{5.2c}$$

$$A - \psi + \frac{1}{a}\left[a^2\,\left(B-a\,\dot{E}\right)\right]^{\cdot} = 0 \tag{5.2d}$$

where $\delta\rho_I$ and δp_I, with $I=(\phi,\chi)$, are the perturbations in the energy densities and pressure associated with the two fields ϕ and χ. Further, the quantities δq_I have been defined through

the relation $\delta T^0_{i(I)} = -\partial_i(\delta q_I)$. The last of the above equations follows from the fact that there are no anisotropic stresses present. The components of the perturbed stress-energy tensor of the two fields can be evaluated to be

$$\delta T^0_{0(\phi)} = -\delta\rho_\phi = -\dot{\phi}\,\dot{\delta\phi} + A\,\dot{\phi}^2 - V_\phi\,\delta\phi, \tag{5.3a}$$

$$\delta T^0_{i(\phi)} = -\partial_i\,\delta q_\phi = -\partial_i\left(\dot{\phi}\,\delta\phi\right), \tag{5.3b}$$

$$\delta T^i_{j(\phi)} = \delta p_\phi\,\delta^i_j = \left(\dot{\phi}\,\dot{\delta\phi} - A\,\dot{\phi}^2 - V_\phi\,\delta\phi\right)\,\delta^i_j. \tag{5.3c}$$

and

$$\delta T^0_{0(\chi)} = -\delta\rho_\chi = 3\,U_0\,\dot{\chi}^3\,\dot{\delta\chi} - 3\,A\,U_0\,\dot{\chi}^4, \tag{5.4a}$$

$$\delta T^0_{i(\chi)} = -\partial_i\,\delta q_\chi = \partial_i\left(U_0\,\dot{\chi}^3\,\delta\chi\right), \tag{5.4b}$$

$$\delta T^i_{j(\chi)} = \delta p_\chi\,\delta^i_j = \left(U_0\,A\,\dot{\chi}^4 - U_0\,\dot{\chi}^3\,\dot{\delta\chi}\right)\,\delta^i_j. \tag{5.4c}$$

5.2 Equations governing the perturbations in the scalar fields

The equations of motion describing the perturbations in the fields can be arrived at from the following conservation equation governing the perturbation in the energy density of a specific component (see, for instance, Refs. [76, 77]):

$$\dot{\delta\rho}_I + 3\,H\,\left(\delta\rho_I + \delta p_I\right) - 3\,\left(\rho_I + p_I\right)\dot{\psi} - \nabla^2\left[\left(\frac{\rho_I + p_I}{a}\right)\,B + \frac{\delta q_I}{a^2} - \left(\rho_I + p_I\right)\dot{E}\right] = 0. \tag{5.5}$$

Upon making use of this equation and the above expressions for the components of the perturbed stress-energy tensor, we can obtain the equations of motion governing the Fourier modes, say, $\delta\phi_k$ and $\delta\chi_k$, associated with the perturbations in the two scalar fields to be

$$\ddot{\delta\phi}_k + 3\,H\,\dot{\delta\phi}_k + V_{\phi\phi}\,\delta\phi_k + 2\,V_\phi\,A_k - \dot{\phi}\,\left(\dot{A}_k + 3\,\dot{\psi}_k\right) + \frac{k^2}{a^2}\,\left[\delta\phi_k + a\,\dot{\phi}\,\left(B_k - a\,\dot{E}_k\right)\right] = 0, \tag{5.6a}$$

$$\ddot{\delta\chi}_k + H\,\dot{\delta\chi}_k - \dot{\chi}\left(\dot{A}_k + \dot{\psi}_k\right) + \frac{k^2}{3\,a^2}\left[\delta\chi_k + a\,\dot{\chi}\,\left(B_k - a\,\dot{E}_k\right)\right] = 0, \tag{5.6b}$$

where, evidently, A_k, B_k, ψ_k and E_k denote the Fourier modes that describe the corresponding metric perturbations. The gauge invariant perturbations associated with the two scalar fields can be constructed to be

$$\overline{\delta\phi}_k = \delta\phi_k + \frac{\dot{\phi}}{H}\,\psi_k, \tag{5.7a}$$

$$\overline{\delta\chi}_k = \delta\chi_k + \frac{\dot{\chi}}{H}\,\psi_k. \tag{5.7b}$$

Upon using the equations of motion (5.6) and the first order Einstein equations (5.2), we find that these gauge invariant perturbations of the two scalar fields obey the following equations:

$$\overline{\delta\phi}_k'' + 2\,\mathcal{H}\,\overline{\delta\phi}_k' + \left(k^2 + a^2\,V_{\phi\phi} + \frac{2\,a^2\,\phi'\,V_\phi}{\mathcal{H}\,M_{_{\rm Pl}}^2} + \frac{3\,\phi'^2}{M_{_{\rm Pl}}^2} - \frac{\phi'^4}{2\,\mathcal{H}^2\,M_{_{\rm Pl}}^4} + \frac{U_0\,\phi'^2\,\chi'^4}{a^2\,\mathcal{H}^2\,M_{_{\rm Pl}}^4}\right)\overline{\delta\phi}_k$$
$$= \frac{U_0\,\phi'\,\chi'^3}{a^2\,\mathcal{H}\,M_{_{\rm Pl}}^2}\,\overline{\delta\chi}_k' + \left(\frac{U_0\,V_\phi\,\chi'^3}{\mathcal{H}\,M_{_{\rm Pl}}^2} + \frac{3\,U_0\,\phi'\,\chi'^3}{a^2\,M_{_{\rm Pl}}^2} - \frac{U_0\,\phi'^3\,\chi'^3}{2\,a^2\,\mathcal{H}^2\,M_{_{\rm Pl}}^4} + \frac{U_0^2\,\phi'\,\chi'^7}{a^4\,\mathcal{H}^2\,M_{_{\rm Pl}}^4}\right)\overline{\delta\chi}_k, \tag{5.8a}$$

$$\overline{\delta\chi}_k'' + \left(\frac{k^2}{3} - \frac{2\,U_0\,\chi'^4}{a^2\,M_{_{\rm Pl}}^2} + \frac{U_0\,\phi'^2\,\chi'^4}{3\,a^2\,\mathcal{H}^2\,M_{_{\rm Pl}}^4} - \frac{U_0^2\,\chi'^8}{2\,a^4\,\mathcal{H}^2\,M_{_{\rm Pl}}^4}\right)\overline{\delta\chi}_k$$
$$= \frac{\phi'\,\chi'}{3\,\mathcal{H}\,M_{_{\rm Pl}}^2}\,\overline{\delta\phi}_k' - \left(\frac{2\,\chi'\,a^2\,V_\phi}{3\,\mathcal{H}\,M_{_{\rm Pl}}^2} + \frac{2\,\phi'\,\chi'}{M_{_{\rm Pl}}^2} - \frac{\phi'^3\,\chi'}{3\,\mathcal{H}^2\,M_{_{\rm Pl}}^4} + \frac{U_0\,\phi'\,\chi'^5}{2\,a^2\,\mathcal{H}^2\,M_{_{\rm Pl}}^4}\right)\overline{\delta\phi}_k. \tag{5.8b}$$

Let us now turn to the construction of the gauge invariant curvature and isocurvature perturbations associated with the two fields. In due course, we shall make use of the above equations to obtain the equations governing the curvature and isocurvature perturbations.

5.3 Constructing the curvature and isocurvature perturbations

As is well known, in the presence of more than one field or fluid, apart from the curvature perturbation, isocurvature perturbations are also generated. The isocurvature perturbations source the curvature perturbations. It is the structure of the complete action describing the matter fields that determines the relation between the perturbations in the fields and the curvature and isocurvature perturbations. While the fluctuations along the direction of the background trajectory in the field space are referred to as the adiabatic or the curvature perturbation, the perturbations along a direction perpendicular to the background trajectory are called the non-adiabatic, entropic or isocurvature perturbations [76–78].

The Lagrangian density associated with the action (4.1) is evidently given by

$$\mathcal{L} = X^{_{\phi\phi}} - V(\phi) - U_0\left(X^{_{\chi\chi}}\right)^2. \tag{5.9}$$

Let us now define a set of basis vectors along the direction of background evolution, *viz.* the adiabatic basis, and another set of basis vectors along the direction perpendicular to the background evolution, which is referred to as the entropic basis. These two sets of basis vectors obey the following orthonormality condition (see, for instance, Refs. [79, 80]):

$$\mathcal{L}_{_{X^{IJ}}}\,e_n^I\,e_m^J = \delta_{nm}, \tag{5.10}$$

where $(I, J) = (\phi, \chi)$, $(n, m) = (1, 2)$ and

$$\mathcal{L}_{_{X^{IJ}}} = \frac{\partial\mathcal{L}}{\partial X^{IJ}}. \tag{5.11}$$

The adiabatic basis vectors can be defined as [79, 80]

$$e_1^I = \frac{\dot{\varphi}^I}{\sqrt{\mathcal{L}_{_{X^{JK}}}\,\dot{\varphi}^J\,\dot{\varphi}^K}}, \tag{5.12}$$

where $(\varphi^1, \varphi^2) = (\phi, \chi)$[2]. Since

$$\mathcal{L}_{_{X^{\phi\phi}}} = 1 \tag{5.13}$$

[2]Actually, since I already represents ϕ and χ, the introduction of φ^I implying $(\varphi^1, \varphi^2) = (\phi, \chi)$ may be considered as redundant notation. However, representing the perturbations in the scalar fields as $\delta\varphi^I = (\delta\phi, \delta\chi)$ seems to be a better choice than denoting them as δI!

and

$$\mathcal{L}_{X^{\chi\chi}} = -2\,U_0\,X^{\chi\chi} = -U_0\,\dot{\chi}^2, \tag{5.14}$$

we can define the two adiabatic basis vectors to be

$$e_1^{\phi} = \frac{\dot{\phi}}{\sqrt{\dot{\phi}^2 - U_0\,\dot{\chi}^4}}, \tag{5.15a}$$

$$e_1^{\chi} = \frac{\dot{\chi}}{\sqrt{\dot{\phi}^2 - U_0\,\dot{\chi}^4}}. \tag{5.15b}$$

The curvature perturbation can be defined in terms of these basis vectors as

$$\mathcal{R} = \frac{H}{\mathcal{L}_{X^{IJ}}\,\dot{\varphi}^I\,\dot{\varphi}^J}\,\mathcal{L}_{X^{KL}}\,\dot{\varphi}^K\,\overline{\delta\varphi}^L = \frac{H}{\sqrt{\mathcal{L}_{X^{IJ}}\,\dot{\varphi}^I\,\dot{\varphi}^J}}\,\mathcal{L}_{X^{KL}}\,e_1^K\,\overline{\delta\varphi}^L, \tag{5.16}$$

where $\overline{\delta\varphi}^L$ is the gauge invariant perturbation associated with the field φ^L. For our model, the curvature perturbation can be constructed to be

$$\mathcal{R} = \frac{H}{\dot{\phi}^2 - U_0\,\dot{\chi}^4}\left(\dot{\phi}\,\overline{\delta\phi} - U_0\,\dot{\chi}^3\,\overline{\delta\chi}\right). \tag{5.17}$$

It is well known that, when multiple components (fluids and/or fields) are present, the total curvature perturbation is defined as (see, for instance, Refs. [76, 77])

$$\mathcal{R} = \sum_I \frac{\rho_I + p_I}{\rho + p}\,\mathcal{R}_I, \tag{5.18}$$

where $\mathcal{R}_I$ is the curvature perturbation associated with an individual component and is given by

$$\mathcal{R}_I = \psi + \frac{H}{\rho_I + p_I}\,\delta q_I. \tag{5.19}$$

For our system, it is easy to show that, if we make use of the expressions for the various quantities we have obtained earlier, the definition (5.18) for the total curvature perturbation indeed matches the explicitly gauge invariant expression (5.17) we have arrived at. Note that the expression (5.17) for $\mathcal{R}$ suggests that it may diverge when $\dot{\phi}^2 - U_0\,\dot{\chi}^4 = 0$, which corresponds to the condition $\dot{H} = 0$. Recall that, $\dot{H} = 0$ at $\mp\eta_* = \mp\eta_0/\sqrt{3}$. As we shall see, the curvature perturbation indeed diverges at these times. The expression (5.17) also suggests that the curvature perturbation may turn out to be zero at the bounce, wherein $H = 0$. However, we find that this actually does not occur at the bounce, but the curvature perturbation vanishes for an instant between the bounce and η_*.

Let us now construct the corresponding basis vectors for the entropic perturbations, *viz.* e_2^{ϕ} and e_2^{χ}. Using Eqs. (5.15) and the orthonormality condition (5.10), we obtain that

$$e_2^{\phi} = \frac{\dot{\chi}\,\sqrt{-U_0\,\dot{\chi}^2}}{\sqrt{\dot{\phi}^2 - U_0\,\dot{\chi}^4}}, \tag{5.20a}$$

$$e_2^{\chi} = \frac{\dot{\phi}}{\sqrt{-U_0\,\dot{\chi}^2}\sqrt{\dot{\phi}^2 - U_0\,\dot{\chi}^4}}. \tag{5.20b}$$

It is straightforward to check that these two basis vectors are indeed orthogonal to the direction of the background evolution. The isocurvature perturbation can therefore be defined in terms of the basis vectors (5.20) as

$$\mathcal{S} = \frac{H}{\sqrt{\mathcal{L}_{_{X^{IJ}}}\,\dot{\varphi}^I\,\dot{\varphi}^J}}\,\mathcal{L}_{_{X^{KL}}}\,e_2^K\,\overline{\delta\varphi}^L. \tag{5.21}$$

This can be expressed as

$$\mathcal{S} = \frac{H\,\sqrt{U_0\,\dot{\chi}^2}}{\dot{\phi}^2 - U_0\,\dot{\chi}^4}\,\left(\dot{\chi}\,\overline{\delta\phi} - \dot{\phi}\,\overline{\delta\chi}\right), \tag{5.22}$$

where, in order for $\mathcal{S}$ to remain a real quantity, we have dropped the minus sign under the square root that appears as an overall coefficient. It is easy to check that, apart from an overall background factor, the isocurvature perturbation we have defined above can be expressed as the difference of the curvature perturbation $\mathcal{R}_I$ [cf. Eq. (5.19)] associated with the two individual fields [76]. Note that, as in the case of the curvature perturbation, the isocurvature perturbation can be expected to diverge at $\mp\eta_*$ and vanish at the bounce. We shall see later that these expectations indeed prove to be true.

5.4 Equations governing the curvature and the isocurvature perturbations

Let $\mathcal{R}_k$ and $\mathcal{S}_k$ denote the Fourier modes associated with the curvature and the isocurvature perturbations. The expressions for the curvature and the isocurvature perturbations we have obtained above can be inverted to arrive at the following relations:

$$\overline{\delta\phi}_k = \frac{1}{\mathcal{H}}\,\left(\phi'\,\mathcal{R}_k - \frac{1}{a}\,\sqrt{U_0\,\chi'^4}\,\mathcal{S}_k\right), \tag{5.23a}$$

$$\overline{\delta\chi}_k = \frac{1}{\mathcal{H}}\,\left(\chi'\,\mathcal{R}_k - \frac{a\,\phi'}{\sqrt{U_0\,\chi'^2}}\,\mathcal{S}_k\right). \tag{5.23b}$$

Using the equations of motion for the gauge invariant field perturbations (5.8), we obtain the equations governing $\mathcal{R}_k$ and $\mathcal{S}_k$ to be

$$\begin{aligned}
&\mathcal{R}_k'' + \left\{\frac{2\,\left(\mathcal{H}'-\mathcal{H}^2\right)}{\mathcal{H}} - 2\,\mathcal{H} + \frac{a}{M_{_{\rm Pl}}^2}\,\left[\frac{2\,\phi'^2}{3\,a\,\mathcal{H}} - \frac{a\,V_\phi\,\phi'}{\mathcal{H}'-\mathcal{H}^2} - \frac{\mathcal{H}\,\phi'^2}{a\,\left(\mathcal{H}'-\mathcal{H}^2\right)}\right]\right.\\
&\qquad\left. - \frac{\phi'^4}{3\,M_{_{\rm Pl}}^4\,\mathcal{H}\,\left(\mathcal{H}'-\mathcal{H}^2\right)}\right\}\mathcal{R}_k' + \frac{k^2}{3}\,\left[1 + \frac{\phi'^2}{M_{_{\rm Pl}}^2\,\left(\mathcal{H}'-\mathcal{H}^2\right)}\right]\mathcal{R}_k\\
&\quad = \frac{\sqrt{U_0\,\chi'^4}\,\phi'}{M_{_{\rm Pl}}^2\,\left(\mathcal{H}'-\mathcal{H}^2\right)}\,\left[\frac{a\,V_\phi}{\phi'} + \frac{\mathcal{H}}{a} - \frac{1}{2\,M_{_{\rm Pl}}^2\,\mathcal{H}}\,\left(\frac{\phi'^2}{a} - \frac{U_0\,\chi'^4}{3\,a^3}\right)\right]\mathcal{S}_k'\\
&\qquad + \frac{\sqrt{U_0\,\chi'^4}\,\phi'}{a\,M_{_{\rm Pl}}^2}\,\left[\frac{k^2}{3\,\left(\mathcal{H}'-\mathcal{H}^2\right)} + \frac{5}{3} + \frac{5\,a^2\,V_\phi}{\mathcal{H}\,\phi'} - \frac{2\,\mathcal{H}^2}{\mathcal{H}'-\mathcal{H}^2} + \frac{V_{\phi\phi}\,a^2}{\mathcal{H}'-\mathcal{H}^2} - \frac{\mathcal{H}'-\mathcal{H}^2}{3\,\mathcal{H}^2}\right.\\
&\qquad\left. + \frac{1}{M_{_{\rm Pl}}^2}\,\left(\frac{2\,V_\phi\,\phi'\,a^2}{3\,\mathcal{H}\,\left(\mathcal{H}'-\mathcal{H}^2\right)} + \frac{\phi'^2}{\mathcal{H}'-\mathcal{H}^2} - \frac{\phi'^2}{3\,\mathcal{H}^2}\right)\right]\mathcal{S}_k, \qquad (5.24a)\\
&\mathcal{S}_k'' + \left[\frac{2\,\left(\mathcal{H}'-\mathcal{H}^2\right)}{\mathcal{H}} - 2\,\mathcal{H} - \frac{1}{M_{_{\rm Pl}}^2}\left(\frac{2\,\phi'^2}{3\,\mathcal{H}} + \frac{V_\phi\,\phi'\,a^2}{\mathcal{H}'-\mathcal{H}^2} + \frac{\mathcal{H}\,\phi'^2}{\mathcal{H}'-\mathcal{H}^2}\right) + \frac{\phi'^4}{3\,M_{_{\rm Pl}}^4\,\mathcal{H}\,\left(\mathcal{H}'-\mathcal{H}^2\right)}\right]\mathcal{S}_k'\\
&\quad + \left\{k^2\,\left[1 - \frac{\phi'^2}{3\,M_{_{\rm Pl}}^2\,\left(\mathcal{H}'-\mathcal{H}^2\right)}\right] - 2\,\mathcal{H}^2 + a^2\,V_{\phi\phi} + \frac{2\,\left(\mathcal{H}'-\mathcal{H}^2\right)^2}{\mathcal{H}^2} - 3\,\left(\mathcal{H}'-\mathcal{H}^2\right)\right.\\
&\qquad + \frac{1}{M_{_{\rm Pl}}^2}\,\left[\frac{2\,\mathcal{H}^2\,\phi'^2}{\mathcal{H}'-\mathcal{H}^2} - \frac{2\,V_\phi\,\phi'\,a^2}{3\,\mathcal{H}} - \frac{2\,\phi'^2}{3} - \frac{V_{\phi\phi}\,\phi'^2\,a^2}{\mathcal{H}'-\mathcal{H}^2} - \frac{2\,\phi'^2\,\left(\mathcal{H}'-\mathcal{H}^2\right)}{3\,\mathcal{H}^2}\right]\\
&\qquad\left. + \frac{1}{M_{_{\rm Pl}}^4}\,\left[\frac{\phi'^4}{3\,\mathcal{H}^2} - \frac{2\,V_\phi\,\phi'^3\,a^2}{3\,\mathcal{H}\,\left(\mathcal{H}'-\mathcal{H}^2\right)} - \frac{2\,\phi'^4}{3\,\left(\mathcal{H}'-\mathcal{H}^2\right)}\right]\right\}\mathcal{S}_k\\
&\quad = \frac{\sqrt{U_0\,\chi'^4}\,\phi'}{M_{_{\rm Pl}}^2\,\left(\mathcal{H}'-\mathcal{H}^2\right)}\left(\frac{\mathcal{H}'-\mathcal{H}^2}{a\,\mathcal{H}} - \frac{\mathcal{H}}{a} - \frac{a\,V_\phi}{\phi'} - \frac{\phi'^2}{3\,M_{_{\rm Pl}}^2\,a\,\mathcal{H}}\right)\mathcal{R}_k' + \frac{\sqrt{U_0\,\chi'^4}\,\phi'}{3\,a\,M_{_{\rm Pl}}^2\,\left(\mathcal{H}'-\mathcal{H}^2\right)}\,k^2\,\mathcal{R}_k. \qquad (5.24b)
\end{aligned}$$

We should stress here that these equations apply to the two field model described by the action (4.1). For the specific bouncing scenario of our interest characterized by the scale factor (2.2), these equations simplify to be

$$\begin{aligned}
&\mathcal{R}_k'' + \frac{2\,\left(7 + 9\,k_0^2\,\eta^2 - 6\,k_0^4\,\eta^4\right)}{\eta\,\left(1 - 3\,k_0^2\,\eta^2\right)\,\left(1 + k_0^2\,\eta^2\right)}\,\mathcal{R}_k' - \frac{k^2\,\left(5 + 9\,k_0^2\,\eta^2\right)}{3\,\left(1 - 3\,k_0^2\,\eta^2\right)}\,\mathcal{R}_k\\
&\quad = \frac{4\,\left(5 + 12\,k_0^2\,\eta^2\right)}{\sqrt{3}\,\eta\,\left(1 - 3\,k_0^2\,\eta^2\right)\,\sqrt{1 + k_0^2\,\eta^2}}\,\mathcal{S}_k' - \frac{4\,\left[5 - 22\,k_0^2\,\eta^2 - 24\,k_0^4\,\eta^4 + k^2\,\eta^2\,\left(1 + k_0^2\,\eta^2\right)^2\right]}{\sqrt{3}\,\eta^2\,\left(1 + k_0^2\,\eta^2\right)^{3/2}\,\left(1 - 3\,k_0^2\,\eta^2\right)}\,\mathcal{S}_k, \qquad (5.25a)\\
&\mathcal{S}_k'' - \frac{2\,\left(9 + 7\,k_0^2\,\eta^2 + 6\,k_0^4\,\eta^4\right)}{\eta\,\left(1 - 3\,k_0^2\,\eta^2\right)\,\left(1 + k_0^2\,\eta^2\right)}\,\mathcal{S}_k'\\
&\quad + \frac{18 - 85\,k_0^2\,\eta^2 - 25\,k_0^4\,\eta^4 - 6\,k_0^6\,\eta^6 + k^2\,\eta^2\,\left(3 - k_0^2\,\eta^2\right)\,\left(1 + k_0^2\,\eta^2\right)^2}{\eta^2\,\left(1 - 3\,k_0^2\,\eta^2\right)\,\left(1 + k_0^2\,\eta^2\right)^2}\,\mathcal{S}_k\\
&\quad = -\frac{4\,\sqrt{3}\,\left(3 - 2\,k_0^2\,\eta^2\right)}{\eta\,\sqrt{1 + k_0^2\,\eta^2}\,\left(1 - 3\,k_0^2\,\eta^2\right)}\,\mathcal{R}_k' + \frac{4\,k^2\,\sqrt{1 + k_0^2\,\eta^2}}{\sqrt{3}\,\left(1 - 3\,k_0^2\,\eta^2\right)}\,\mathcal{R}_k. \qquad (5.25b)
\end{aligned}$$

Note that the denominators of some of the coefficients in these equations contain either a factor of η or $(1 - 3\,k_0^2\,\eta^2)$. Therefore, as one approaches the bounce during the contracting phase, the coefficients will first diverge at $-\eta_*$ and then at the bounce. Later, after the bounce, they will also diverge at η_*, before we get to evaluate the power spectra. Due to this reason, the above equations do not permit us to evolve the quantities $\mathcal{R}_k$ and $\mathcal{S}_k$ across the bounce. This issue can be circumvented by working in a specific gauge and considering two other suitable quantities to characterize the perturbations whose governing equations remain well behaved around the bounce (see Ref. [30], in this context, also see Ref. [81]).

Another related point needs to be emphasized at this stage of our discussion. As we shall describe in some detail in the next section, the initial conditions on the perturbations need to be imposed at sufficiently early times when the modes are well inside the Hubble radius during the contracting phase. Moreover, in order to impose the standard initial conditions on the curvature and isocurvature perturbations, the modes need to be decoupled during these early times. It has been pointed out that a strong coupling between the two modes would not permit the imposition of standard, independent initial conditions on the modes (for a detailed discussion on this issue, see Ref. [82]). In due course, we shall discuss the specific initial conditions that we shall impose on the perturbations (see Sub-sec. 6.2). We ought to stress here that the Eqs. (5.25) governing $\mathcal{R}_k$ and $\mathcal{S}_k$ indeed decouple at very early times, *i.e.* as $\eta \to -\infty$ [cf. Eqs. (6.3) and (6.4)]. We should highlight the fact that, in the next two sections, apart from the numerical solutions, we shall also construct analytical solutions, which we shall show match the numerical results very well.

5.5 Perturbations in a specific gauge

We now need to identify a suitable gauge wherein the perturbations can be evolved across the bounce without facing the difficulties mentioned above. We find that these difficulties can be avoided if we choose to work in the uniform-χ gauge [30]. In this gauge, the two independent scalar perturbations turn out to be the metric potentials A and ψ and, as we shall soon illustrate, these quantities can be smoothly evolved across the bounce. The curvature and the isocurvature perturbations can then be suitably constructed from these two scalar perturbations.

The uniform χ-gauge corresponds to the situation wherein $\delta\chi_k = 0$. In such a case, Eq. (5.6b) reduces to

$$\frac{k^2}{3\,a}\left(B_k - a\,\dot{E}_k\right) = \left(\dot{A}_k + \dot{\psi}_k\right). \tag{5.26}$$

Upon using this relation, the first order Einstein equations (5.2) and the background equations, we obtain the following equations governing A_k and ψ_k:

$$A_k'' + 4\,\mathcal{H}\,A_k' + \left[\frac{k^2}{3} - \left(6\,\mathcal{H}^2 - \frac{\phi'^2}{M_{_{\rm Pl}}^2} + \frac{2\,a^2\,\mathcal{H}\,V_\phi}{\phi'} + \frac{2\,U_0\,\chi'^4}{a^2\,M_{_{\rm Pl}}^2}\right)\right] A_k = \frac{2\,a^2\,V_\phi}{\phi'}\,\psi_k' + \frac{4\,k^2}{3}\,\psi_k, \tag{5.27a}$$

$$\psi_k'' + \left(2\,\mathcal{H} + \frac{2\,a^2\,V_\phi}{\phi'}\right)\psi_k' + k^2\,\psi_k = 2\,\mathcal{H}\,A_k' - \left(6\,\mathcal{H}^2 - \frac{\phi'^2}{M_{_{\rm Pl}}^2} + \frac{2\,a^2\,\mathcal{H}\,V_\phi}{\phi'} + \frac{2\,U_0\,\chi'^4}{a^2\,M_{_{\rm Pl}}^2}\right) A_k. \tag{5.27b}$$

We should again mention that these equations correspond to the system described by the action (4.1). For the specific bouncing scenario that we are considering here, the above

equations simplify to

$$A_k'' + 4\,\mathcal{H}\,A_k' + \left(\frac{k^2}{3} - \frac{20\,a_0^2\,k_0^2}{a^2}\right)\,A_k = -3\,\mathcal{H}\,\psi_k' + \frac{4\,k^2}{3}\,\psi_k, \tag{5.28a}$$

$$\psi_k'' - \mathcal{H}\,\psi_k' + k^2\,\psi_k = 2\,\mathcal{H}\,A_k' - \frac{20\,a_0^2\,k_0^2}{a^2}\,A_k. \tag{5.28b}$$

In arriving at these two equations, we have made use of the relation: $\dot{\phi}^2/2 = V\,(\phi)$, which arises due to the fact that the field ϕ is pressureless. Note that, in the uniform χ-gauge, the curvature and isocurvature perturbations are given by

$$\mathcal{R}_k = \psi_k + \frac{2\,H\,M_{_{\rm Pl}}^2}{\dot{\phi}^2 - U_0\,\dot{\chi}^4}\,\left(\dot{\psi}_k + H\,A_k\right), \tag{5.29a}$$

$$\mathcal{S}_k = \frac{2\,H\,M_{_{\rm Pl}}^2\,\sqrt{U_0\,\dot{\chi}^4}}{\left(\dot{\phi}^2 - U_0\,\dot{\chi}^4\right)\,\dot{\phi}}\,\left(\dot{\psi}_k + H\,A_k\right). \tag{5.29b}$$

Later, we shall make use of these relations to construct $\mathcal{R}_k$ and $\mathcal{S}_k$ from A_k and ψ_k around the bounce.

6 Evolution of the scalar perturbations

Let us now turn to solving the equations governing the scalar perturbations numerically. Since we have analytical solutions to describe the behavior of the background quantities, we need to develop the numerical procedure only for the evolution of the perturbations. Our main aim is to evaluate the scalar power spectra after the bounce, which, obviously, requires us to evolve the perturbations across the bounce. In the case of tensors, we could evolve the perturbations smoothly across the bounce and evaluate the corresponding power spectrum at a suitable time after the bounce. However, in the case of scalars, as we have described above, it does not seem possible to integrate the equations describing the curvature and the isocurvature perturbations across the bounce due to the presence of diverging coefficients. We shall hence choose to evolve the metric perturbations A_k and ψ_k across the bounce, since the equations governing them are devoid of such divergent terms. Once we have evolved A_k and ψ_k across the bounce, we shall reconstruct the curvature and the isocurvature perturbations $\mathcal{R}_k$ and $\mathcal{S}_k$ from these quantities to arrive at the power spectra.

Recall that, in the case of tensors, when evaluating the perturbations *analytically*, we had divided the period of our interest – *i.e.* from very early times during the contracting phase to a suitable time immediately after the bounce – into two domains, *viz.* $-\infty < \eta \leq -\alpha\,\eta_0$ and $-\alpha\,\eta_0 \leq \eta \leq \beta\,\eta_0$, where we had set $\alpha = 10^5$ and $\beta = 10^2$. In the case of scalars, we shall work over these two domains to evolve the perturbations *analytically as well as numerically*. In the first domain, we shall identify the Mukhanov-Sasaki variables associated with the perturbations $\mathcal{R}_k$ and $\mathcal{S}_k$ and impose the corresponding Bunch-Davies initial conditions on these variables at suitably early times. We shall evolve the perturbations $\mathcal{R}_k$ and $\mathcal{S}_k$ using the governing equations (5.25) until $\eta = -\alpha\,\eta_0$. At $\eta = -\alpha\,\eta_0$, we shall match the quantities $\mathcal{R}_k$ and $\mathcal{S}_k$ (and their time derivatives) to the metric perturbations A_k and ψ_k (and their time derivatives) using the relations (5.29). Thereafter, we shall evolve the perturbations A_k and ψ_k [using Eqs. (5.28)] until $\eta = \beta\,\eta_0$ after the bounce. Once we have evolved A_k and ψ_k across the bounce, we can reconstruct the quantities $\mathcal{R}_k$ and $\mathcal{S}_k$ [using Eqs. (5.29)] and also, eventually, evaluate their power spectra.

6.1 Equations in terms of e-$\mathcal{N}$-folds

As in the case of tensors, we shall numerically integrate the equations with e-$\mathcal{N}$-folds as the independent variable. We need to numerically integrate the equations governing the evolution of the quantities $\mathcal{R}_k$, $\mathcal{S}_k$, ψ_k and A_k. In terms of the variable e-$\mathcal{N}$-folds, Eqs. (5.25) can be written as

$$\begin{aligned}
&\frac{\mathrm{d}^2\mathcal{R}_k}{\mathrm{d}\mathcal{N}^2} + \left[\mathcal{N} + \frac{1}{H}\frac{\mathrm{d}H}{\mathrm{d}\mathcal{N}} - \frac{1}{\mathcal{N}} + \frac{2\,a_0\,\mathcal{N}}{a^2\,H\,\eta}\left(\frac{7 + 9\,k_0^2\,\eta^2 - 6\,k_0^4\,\eta^4}{1 - 3\,k_0^2\,\eta^2}\right)\right]\frac{\mathrm{d}\mathcal{R}_k}{\mathrm{d}\mathcal{N}} \\
&\quad - \frac{k^2\,\mathcal{N}^2}{3\,a^2\,H^2}\left(\frac{5 + 9\,k_0^2\,\eta^2}{1 - 3\,k_0^2\,\eta^2}\right)\mathcal{R}_k \\
&\quad = \frac{4\,a_0^{1/2}\,\mathcal{N}}{\sqrt{3}\,a^{3/2}\,H\,\eta}\left(\frac{5 + 12\,k_0^2\,\eta^2}{1 - 3\,k_0^2\,\eta^2}\right)\frac{\mathrm{d}\mathcal{S}_k}{\mathrm{d}\mathcal{N}} \\
&\quad\quad - \frac{4\,\mathcal{N}^2\,a_0^{3/2}}{\sqrt{3}\,a^{7/2}\,H^2\,\eta^2}\left[\frac{5 - 22\,k_0^2\,\eta^2 - 24\,k_0^4\,\eta^4 + k^2\,\eta^2\,(a/a_0)^2}{1 - 3\,k_0^2\,\eta^2}\right]\mathcal{S}_k, \qquad (6.1a) \\
&\frac{\mathrm{d}^2\mathcal{S}_k}{\mathrm{d}\mathcal{N}^2} + \left[\mathcal{N} + \frac{1}{H}\frac{\mathrm{d}H}{\mathrm{d}\mathcal{N}} - \frac{1}{\mathcal{N}} - \frac{2\,a_0\,\mathcal{N}}{a^2\,H\,\eta}\left(\frac{9 + 7\,k_0^2\,\eta^2 + 6\,k_0^4\,\eta^4}{1 - 3\,k_0^2\,\eta^2}\right)\right]\frac{\mathrm{d}\mathcal{S}_k}{\mathrm{d}\mathcal{N}} \\
&\quad + \frac{a_0^2\,\mathcal{N}^2}{a^4\,H^2\,\eta^2}\left(\frac{18 - 85\,k_0^2\,\eta^2 - 25\,k_0^4\,\eta^4 - 6\,k_0^6\,\eta^6 + k^2\,\eta^2\,(3 - k_0^2\,\eta^2)\,(a/a_0)^2}{1 - 3\,k_0^2\,\eta^2}\right)\mathcal{S}_k \\
&\quad = -\frac{4\,\sqrt{3}\,a_0^{1/2}\,\mathcal{N}}{a^{3/2}\,H\,\eta}\left(\frac{3 - 2\,k_0^2\,\eta^2}{1 - 3\,k_0^2\,\eta^2}\right)\frac{\mathrm{d}\mathcal{R}_k}{\mathrm{d}\mathcal{N}} + \frac{4\,k^2\,\mathcal{N}^2}{\sqrt{3}\,a_0^{1/2}\,a^{3/2}\,H^2}\left(\frac{1}{1 - 3\,k_0^2\,\eta^2}\right)\mathcal{R}_k. \qquad (6.1b)
\end{aligned}$$

Similarly, we find that Eqs. (5.28) can be expressed as

$$\begin{aligned}
&\frac{\mathrm{d}^2 A_k}{\mathrm{d}\mathcal{N}^2} + \left(5\,\mathcal{N} + \frac{1}{H}\frac{\mathrm{d}H}{\mathrm{d}\mathcal{N}} - \frac{1}{\mathcal{N}}\right)\frac{\mathrm{d}A_k}{\mathrm{d}\mathcal{N}} + \left(\frac{k^2\,\mathcal{N}^2}{3\,a^2\,H^2} - \frac{20\,a_0^2\,\mathcal{N}^2\,k_0^2}{a^4\,H^2}\right)A_k \\
&\qquad = -3\,\mathcal{N}\frac{\mathrm{d}\psi_k}{\mathrm{d}\mathcal{N}} + \frac{4\,k^2\,\mathcal{N}^2}{3\,a^2\,H^2}\,\psi_k, \qquad (6.2a) \\
&\frac{\mathrm{d}^2\psi_k}{\mathrm{d}\mathcal{N}^2} + \left(\frac{1}{H}\frac{\mathrm{d}H}{\mathrm{d}\mathcal{N}} - \frac{1}{\mathcal{N}}\right)\frac{\mathrm{d}\psi_k}{\mathrm{d}\mathcal{N}} + \frac{k^2\,\mathcal{N}^2}{a^2\,H^2}\,\psi_k \\
&\qquad = 2\,\mathcal{N}\frac{\mathrm{d}A_k}{\mathrm{d}\mathcal{N}} - \frac{20\,a_0^2\,\mathcal{N}^2\,k_0^2}{a^4\,H^2}\,A_k. \qquad (6.2b)
\end{aligned}$$

In the above equations, to avoid rather lengthy and cumbersome expressions, we have not attempted to express the coefficients involving the conformal time coordinate in terms of e-$\mathcal{N}$-folds.

6.2 Initial conditions and power spectra

Let us now understand the initial conditions that need to be imposed on the scalar perturbations. Note that, at very early times during the contracting phase, the energy density of the canonical scalar field ϕ dominates the energy density of the non-canonical field χ. In inflationary scenarios driven by two fields, it is well known that, when the background is largely driven by one of the two fields, the isocurvature perturbation can be neglected [78]. This seems to suggest that we can ignore the effect of the isocurvature perturbation on the

curvature perturbation at early times. In such a case, we find that the equation (5.25a) governing the curvature perturbation simplifies to be

$$\mathcal{R}_k'' + 2\,\frac{z'}{z}\,\mathcal{R}_k' + k^2\,\mathcal{R}_k \simeq 0, \tag{6.3}$$

where $z \simeq a\,\dot{\phi}/H$, which simplifies to $z \simeq \sqrt{3}\,M_{_{\rm Pl}}\,a$ in the particular matter bounce scenario that we are considering.

In an expanding universe, we can expect the isocurvature perturbations to decay and, hence, they are not expected to play a significant role at late times. However, since perturbations can grow in a contracting universe, the effect of the isocurvature perturbations may not be negligible as one approaches the bounce. Therefore, though the effects of the isocurvature perturbations may be insignificant at early times, their contribution may need to be accounted for as one approaches the bounce, particularly when the energy density of the second field χ becomes comparable to the energy density of the ϕ field. At early times, we find that the curvature and the isocurvature perturbations decouple, and the equation (5.25b) describing the isocurvature perturbation simplifies to

$$\mathcal{S}_k'' + 2\,\frac{z'}{z}\,\mathcal{S}_k' + \left(\frac{k^2}{3} + \frac{\phi'^2}{6\,M_{_{\rm Pl}}^2}\right)\,\mathcal{S}_k \simeq 0. \tag{6.4}$$

Let us define the Mukhanov-Sasaki variable corresponding to the perturbations $\mathcal{R}_k$ and $\mathcal{S}_k$ to be $\mathcal{U}_k = z\,\mathcal{R}_k$ and $\mathcal{V}_k = z\,\mathcal{S}_k$, where $z = a\,\dot{\phi}/H$. In terms of these variables, in the matter bounce scenario of our interest, the above two decoupled equations for $\mathcal{R}_k$ and $\mathcal{S}_k$ reduce to

$$\mathcal{U}_k'' + \left(k^2 - \frac{2}{\eta^2}\right)\,\mathcal{U}_k \simeq 0, \tag{6.5a}$$

$$\mathcal{V}_k'' + \frac{k^2}{3}\,\mathcal{V}_k \simeq 0. \tag{6.5b}$$

It is useful to note that, in the matter dominated phase, the mode $\mathcal{U}_k$ behaves exactly as the Mukhanov-Sasaki variable u_k corresponding to the tensor perturbation. At very early times, *i.e.* when $k^2 \gg 2/\eta^2$, we can impose the following Bunch-Davies initial conditions on these variables:

$$\mathcal{U}_k = \frac{1}{\sqrt{2\,k}}\,{\rm e}^{-i\,k\,\eta}, \tag{6.6a}$$

$$\mathcal{V}_k = \frac{3^{1/4}}{\sqrt{2\,k}}\,{\rm e}^{-i\,k\,\eta/\sqrt{3}}. \tag{6.6b}$$

These initial conditions can evidently be translated to the corresponding initial conditions on $\mathcal{R}_k$ and $\mathcal{S}_k$ and their derivatives with respect to the e-$\mathcal{N}$-fold.

During early times, when the initial conditions are imposed, the curvature and the isocurvature perturbations are considered to be statistically independent quantities. Therefore, as is usually done in the case of two field models, we shall numerically integrate the equations (6.1) using two sets of initial conditions (in this context, see, for instance, Refs. [83, 84]). In the first case, we perform the integration by imposing the Bunch-Davies initial condition corresponding to (6.6a) on $\mathcal{R}_k$ and setting the initial value of $\mathcal{S}_k$ to be zero. While, in the

second case, we impose the initial condition corresponding to (6.6b) on $\mathcal{S}_k$ and set the initial value of $\mathcal{R}_k$ to be zero. Let us denote the perturbations $\mathcal{R}_k$ and $\mathcal{S}_k$ evolved according to these two sets of initial conditions to be $(\mathcal{R}_k^{\rm I}, \mathcal{S}_k^{\rm I})$ and $(\mathcal{R}_k^{\rm II}, \mathcal{S}_k^{\rm II})$, respectively. Then, the power spectra associated with the curvature and the isocurvature perturbations can be defined as [83, 84]

$$\mathcal{P}_{\mathcal{R}}(k) = \frac{k^3}{2\,\pi^2}\left(\left|\mathcal{R}_k^{\rm I}\right|^2 + \left|\mathcal{R}_k^{\rm II}\right|^2\right), \tag{6.7a}$$

$$\mathcal{P}_{\mathcal{S}}(k) = \frac{k^3}{2\,\pi^2}\left(\left|\mathcal{S}_k^{\rm I}\right|^2 + \left|\mathcal{S}_k^{\rm II}\right|^2\right). \tag{6.7b}$$

6.3 Evolution of the perturbations

We impose the initial conditions as we have described above when $k^2 = 10^4\,(a''/a)$[3]. We integrate the equations (6.1) governing $\mathcal{R}_k$ and $\mathcal{S}_k$ from this initial time up to $\eta = -\alpha\,\eta_0$, where, as before, we shall set $\alpha = 10^5$ (which corresponds to an e-$\mathcal{N}$-fold of about $\mathcal{N} \simeq -6.79$). As in the case of tensors, we carry out the numerical integration using a fifth order Runge-Kutta algorithm. Having integrated for $\mathcal{R}_k$ and $\mathcal{S}_k$ until $\mathcal{N} = -6.79$, we evaluate the values of A_k and ψ_k (and their derivatives) at this time by inverting the relations (5.29). Using these as initial conditions, we integrate the equations (6.2) across the bounce until $\eta = \beta\,\eta_0$, with $\beta = 10^2$, which corresponds to $\mathcal{N} = 4.3$. We then reconstruct the evolution of $\mathcal{R}_k$ and $\mathcal{S}_k$ across the bounce using the relations (5.29). In Fig. 3, we have plotted the evolution of curvature perturbation $(\mathcal{R}_k^{\rm I}, \mathcal{R}_k^{\rm II})$ and the isocurvature perturbation $(\mathcal{S}_k^{\rm I}, \mathcal{S}_k^{\rm II})$, arrived at numerically for a specific wavenumber which corresponds to cosmological scales today.

There a few points that needs to be emphasized concerning the results we have obtained. As we have discussed earlier, the curvature and the isocurvature perturbations are expected to diverge at $\eta = \mp\eta_*$, and it is clear from the figure that they indeed do so. Moreover, the isocurvature perturbation vanishes at the bounce, as expected. In contrast, we find that the curvature perturbation does not vanish at the bounce as one may naively guess, but does so a little time after the bounce. This behavior seems to be responsible for the isocurvature perturbation too to vanish a little time later. Note that, as in the case of tensors, the amplitude of the curvature perturbation almost freezes at suitably late times (in fact, after $\eta = \eta_*$) during the expanding phase. During the period, the isocurvature perturbations begin to decay. As we shall illustrate later, this leads to a strongly adiabatic scalar power spectrum, with the amplitude of the isocurvature perturbations being much smaller than the curvature perturbations.

7 Analytical arguments

In this section, we shall arrive at analytical solutions for the curvature and isocurvature perturbations for scales of cosmological interest under well-motivated approximations. We shall again divide the period of interest into two domains, as we have discussed already. Let us go on to construct the solutions to the equations governing the scalar perturbations in the two domains.

[3]Note that, at early times, since $z \propto a$, $z''/z = a''/a$. This behavior is indeed expected when the scale factor is described by a power law.

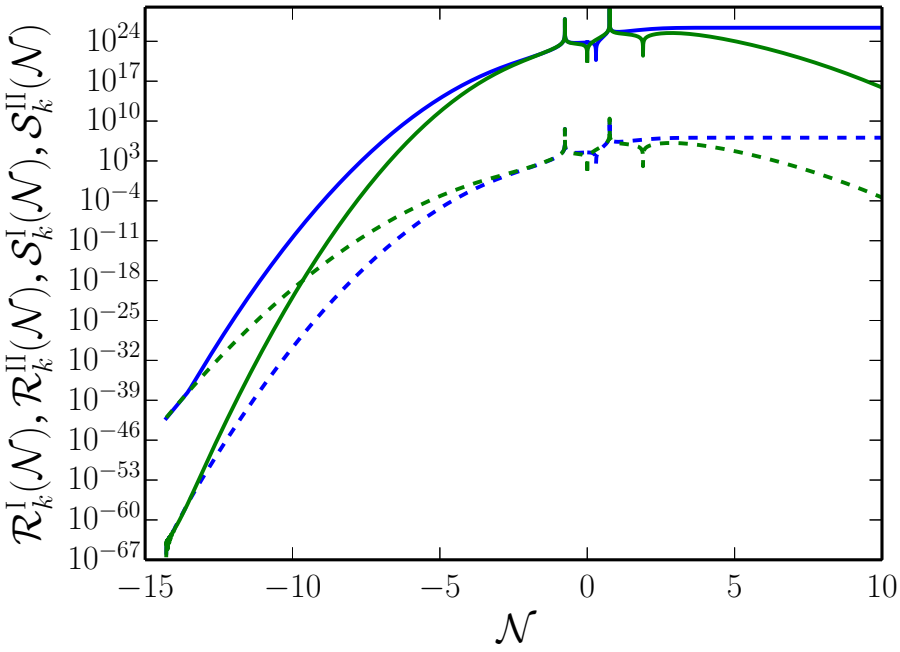

Figure 3. The numerical results for the amplitudes of the curvature (in blue, with $\mathcal{R}_k^{\rm I}$ as solid and $\mathcal{R}_k^{\rm II}$ as dashed) and the isocurvature (in green, with $\mathcal{S}_k^{\rm I}$ as solid and $\mathcal{S}_k^{\rm II}$ as dashed) perturbations evolved with different sets of initial conditions have been plotted as a function of e-$\mathcal{N}$-folds for $k/k_0 = 10^{-20}$. As in Fig. 1, we have set $k_0 = M_{_{\rm Pl}}$ and $a_0 = 3 \times 10^7$, corresponding to $k_0/(a_0\, M_{_{\rm Pl}}) = 3.3 \times 10^{-8}$ which, as we shall see, leads to a scale invariant scalar power spectrum whose amplitude matches COBE normalization [85]. We have plotted the results from the initial e-$\mathcal{N}$-fold $\mathcal{N}_i$ [when $k^2 = 10^4\,(a''/a)$] corresponding to the mode. Note that the amplitudes of $\mathcal{R}_k^{\rm I}$ and $\mathcal{S}_k^{\rm I}$ are dominant (at suitably late times) when compared to that of $\mathcal{R}_k^{\rm II}$ and $\mathcal{S}_k^{\rm II}$, respectively. Also, the curvature perturbation behaves largely in a fashion similar to the tensor perturbation [cf. Fig. 1]. The upward and downward spikes in the plots correspond to points in time where the perturbations diverge and vanish, respectively. As we had expected, both the curvature and the isocurvature perturbations diverge at $\eta = \mp\eta_*$. However, it is only the isocurvature perturbation that vanishes at the bounce. The curvature perturbation actually goes to zero soon after the bounce (during $0 < \eta < \eta_*$), which in turn leads to the vanishing of the isocurvature perturbation a little time later (soon after $\eta = \eta_*$). While the curvature perturbation is largely constant (after $\eta = \eta_*$) during the expanding phase, the isocurvature perturbation begins to decay.

7.1 Solutions in the first domain

As we have discussed before, at early times during the matter dominated contraction, we can assume that the equations governing the evolution of the curvature and the isocurvature perturbations are decoupled. We had mentioned earlier that, during this phase, the mode $\mathcal{U}_k$ is expected to behave exactly like the Mukhanov-Sasaki variable u_k associated with the tensor mode. This is not surprising since such a behavior is well known in power law expansion and, hence, can be expected in power law contraction as well. Using the Bunch-Davies initial condition (6.6a), during sufficiently early times, the solution to Eq. (6.3) can be obtained to be

$$\mathcal{R}_k(\eta) \simeq \frac{1}{\sqrt{6\,k}\, M_{_{\rm Pl}}\, a_0\, k_0^2\, \eta^2} \left(1 - \frac{i}{k\,\eta}\right) \mathrm{e}^{-i\,k\,\eta}, \tag{7.1}$$

which, it should be emphasized, is the same as the solution (3.8) for the tensor mode apart from an overall constant.

Obtaining the solution to the isocurvature perturbation requires a little more care. In arriving at the equation (6.5b) governing the Mukhanov-Sasaki variable associated with the isocurvature perturbation, we had completely ignored the role of the curvature perturbation. While this seems acceptable for determining the initial condition, we find that the effect of the curvature perturbation needs to be accounted for, in order to achieve a better approximation. During the first domain, upon using the expression (7.1) for $\mathcal{R}_k$, we find that the solution to Eq. (5.25b) can be obtained to be [86]

$$\mathcal{S}_k(\eta) \simeq \frac{1}{9\sqrt{2\,k^3}\,a_0\,k_0^3\,M_{_{\rm Pl}}\eta^4}\left(-12\,i\,(1+i\,k\,\eta)\,{\rm e}^{-i\,k\,\eta} + \frac{9}{3^{1/4}}\,k\,k_0\,\eta^2\,{\rm e}^{-i\,k\,\eta/\sqrt{3}} + 4\,k^2\,\eta^2\,{\rm e}^{-i\,k\,\eta/\sqrt{3}}\left\{\pi + i\,{\rm Ei}\left[{\rm e}^{-i\,(3-\sqrt{3})\,k\,\eta/3}\right]\right\}\right), \tag{7.2}$$

where ${\rm Ei}\,[z]$ is the exponential integral function (see, for instance, Ref. [87]). It is straightforward to check that, at early times, it is the second term in the above expression which survives, which exactly corresponds to the initial condition (6.6b).

7.2 Solutions in the second domain

As we have discussed, in the second domain (*i.e.* over the period $-\alpha\,\eta_0 \leq \eta \leq \beta\,\eta_0$), we shall solve for the metric perturbations A_k and ψ_k. In this domain, for scales of cosmological interest, we can ignore the k dependent terms in Eqs. (5.28). Under this condition, the two equations can be combined to obtain that

$$(A_k + \psi_k)'' + 2\,\mathcal{H}\,(A_k + \psi_k)' \simeq 0, \tag{7.3}$$

which is exactly the equation for the tensor mode h_k that we had arrived in this domain [cf. Eq. (3.9)]. This equation can be integrated once to yield

$$(A_k + \psi_k)' \simeq \frac{k_0\,\mathcal{C}_k}{a^2}. \tag{7.4}$$

with $\mathcal{C}_k$ being a constant of integration. Upon further integration, we obtain that

$$A_k(\eta) + \psi_k(\eta) \simeq \frac{\mathcal{C}_k}{2\,a_0^2}\,f(k_0\,\eta) + \mathcal{D}_k, \tag{7.5}$$

where the function f is given by Eq. (3.12) and $\mathcal{D}_k$ is a second constant of integration. Upon substituting this result in Eq. (5.28a), we can arrive at an equation governing A_k. On solving the resulting differential equation (say, using Mathematica [86]), we find that the solution for A_k is given by

$$A_k(\eta) \simeq \frac{\mathcal{C}_k\,k_0\,\eta}{4\,a_0^2\,(1+k_0^2\,\eta^2)} + \mathcal{E}_k\,{\rm e}^{-2\,\sqrt{5}\,\tan^{-1}(k_0\,\eta)} + \mathcal{F}_k\,{\rm e}^{2\,\sqrt{5}\,\tan^{-1}(k_0\,\eta)}, \tag{7.6}$$

where $\mathcal{E}_k$ and $\mathcal{F}_k$ denote two additional constants of integration. The corresponding solution for ψ_k can be obtained by substituting this result in Eq. (7.5).

Having obtained the solutions for A_k and ψ_k, we can now reconstruct the curvature and the isocurvature perturbations $\mathcal{R}_k$ and $\mathcal{S}_k$ using Eqs. (5.29). We find that, in the second domain, $\mathcal{R}_k$ and $\mathcal{S}_k$ are given by

$$\mathcal{R}_k(\eta) \simeq \frac{-1}{2\,a_0^2\,\left(1-2\,k_0^2\,\eta^2-3\,k_0^4\,\eta^4\right)}\Bigg(\mathcal{C}_k\,\Bigg[\left(1+3\,k_0^2\,\eta^2\right)\,k_0\,\eta - \left(1-2\,k_0^2\,\eta^2-3\,k_0^4\,\eta^4\right)\,\tan^{-1}\left(k_0\,\eta\right)\Bigg] - 2\,a_0^2\,\left(1+k_0^2\,\eta^2\right)\,\Bigg[\mathcal{D}_k\,\left(1-3\,k_0^2\,\eta^2\right) - \mathcal{E}_k\,\left(1+2\,\sqrt{5}\,k_0\,\eta-k_0^2\,\eta^2\right)\,\mathrm{e}^{-2\,\sqrt{5}\,\tan^{-1}(k_0\,\eta)} - \mathcal{F}_k\,\left(1-2\,\sqrt{5}\,k_0\,\eta-k_0^2\,\eta^2\right)\,\mathrm{e}^{2\,\sqrt{5}\,\tan^{-1}(k_0\,\eta)}\Bigg]\Bigg\}, \tag{7.7a}$$

$$\mathcal{S}_k(\eta) \simeq \frac{-k_0\,\eta}{2\,\sqrt{3}\,a_0^2\,\left(1+k_0^2\,\eta^2\right)^{1/2}\,\left(1-3\,k_0^2\,\eta^2\right)}\Bigg\{3\,\mathcal{C}_k + 8\,a_0^2\,\Bigg[\mathcal{E}_k\,\left(\sqrt{5}+k_0\,\eta\right)\,\mathrm{e}^{-2\,\sqrt{5}\,\tan^{-1}(k_0\,\eta)} - \mathcal{F}_k\,\left(\sqrt{5}-k_0\,\eta\right)\,\mathrm{e}^{2\,\sqrt{5}\,\tan^{-1}(k_0\,\eta)}\Bigg]\Bigg\}. \tag{7.7b}$$

The four constants $\mathcal{C}_k$, $\mathcal{D}_k$, $\mathcal{E}_k$ and $\mathcal{F}_k$ can be determined by matching these solutions with the solutions for $\mathcal{R}_k$ and $\mathcal{S}_k$ we had obtained in the first domain at $\eta = -\alpha\,\eta_0$. The expressions describing the constants are long and cumbersome and, hence, we relegate the details to an appendix (see App. A).

7.3 Comparison with the numerical results

Let us now compare the above analytical results for $\mathcal{R}_k$ and $\mathcal{S}_k$ with the numerical results. Recall that, numerically, we had obtained two sets of solutions for $\mathcal{R}_k$ and $\mathcal{S}_k$, *viz.* $(\mathcal{R}_k^{\mathrm{I}}, \mathcal{S}_k^{\mathrm{I}})$ and $(\mathcal{R}_k^{\mathrm{II}}, \mathcal{S}_k^{\mathrm{II}})$, corresponding to two different sets of initial conditions. In contrast, while arriving at the analytical results, for convenience, we have imposed the Bunch-Davies initial on both $\mathcal{R}_k$ and $\mathcal{S}_k$ simultaneously. We shall compare the amplitudes of $\mathcal{R}_k$ and $\mathcal{S}_k$ obtained analytically with the amplitudes $\mathcal{R}_k^{\mathrm{I}} + \mathcal{R}_k^{\mathrm{II}}$ and $\mathcal{S}_k^{\mathrm{I}} + \mathcal{S}_k^{\mathrm{II}}$ arrived at numerically. (Recall that, the amplitudes of $\mathcal{R}_k^{\mathrm{I}}$ and $\mathcal{S}_k^{\mathrm{I}}$ had dominated those of $\mathcal{R}_k^{\mathrm{II}}$ and $\mathcal{S}_k^{\mathrm{II}}$, respectively.) In Figs. 4 and 5, we have plotted the analytical and the numerical results for wavenumbers such that $k/k_0 = 10^{-20}$ and $k/k_0 = 10^{-25}$, respectively. As is evident from the figures, the analytical results match the numerical results very well. In fact, we find the difference between the analytical and numerical results to be less than 2%.

8 The scalar power spectra and the tensor-to-scalar ratio

With the analytical and the numerical results at hand, let us now go on to evaluate the scalar power spectra and the tensor-to-scalar ratio. In order to understand the effects of the bounce on these quantities, let us evaluate the scalar and tensor power spectra before as well as after the bounce.

Let us first consider the numerical results, which are exhibited in Fig. 6. All the power spectra are strictly scale invariant (over scales of cosmological interest) before as well as after the bounce. The power spectra before the bounce have been evaluated at $\eta = -\alpha\,\eta_0$, with $\alpha = 10^5$, which, as we had mentioned, corresponds to $\mathcal{N} = -6.79$. The power spectra after

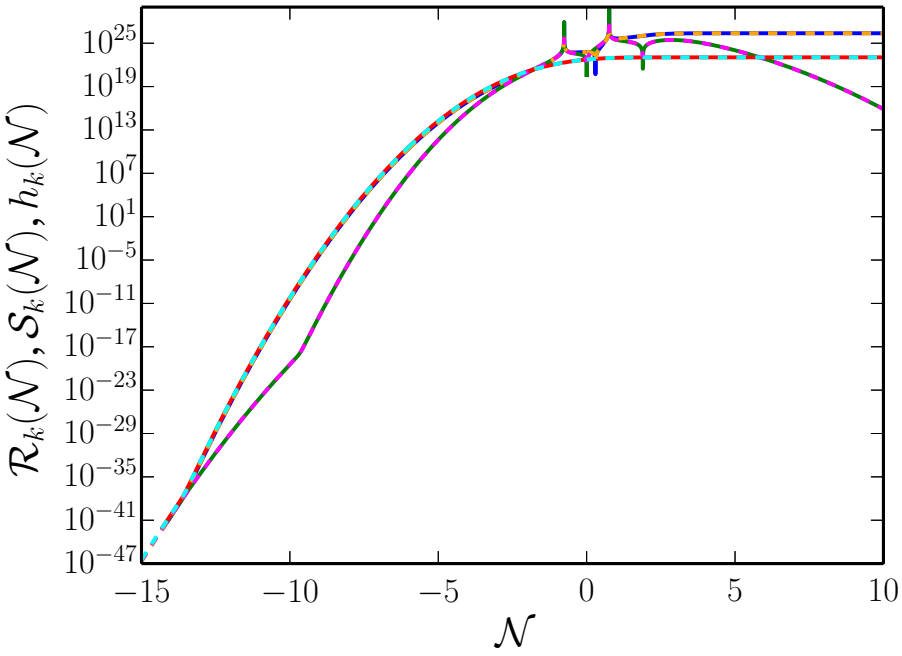

Figure 4. A comparison of the numerical results (solid lines) with the analytical results (dashed lines) for the amplitude of the curvature perturbation $\mathcal{R}_k$ (blue solid line and orange dashed line), the isocurvature perturbation $\mathcal{S}_k$ (green solid line and magenta dashed line) and the tensor mode h_k (red solid line and cyan dashed line) corresponding to the wavenumber $k/k_0 = 10^{-20}$. As earlier, we have set $k_0 = M_{_{\rm Pl}}$ and $a_0 = 3 \times 10^7$, corresponding to $k_0/(a_0\, M_{_{\rm Pl}}) = 3.3 \times 10^{-8}$ and, for plotting the analytical results, we have chosen $\alpha = 10^5$. We have plotted the numerical results from the initial e-$\mathcal{N}$-fold $\mathcal{N}_i$ [when $k^2 = 10^4\,(a''/a)$] corresponding to the mode. Evidently, the analytical and numerical results match extremely well, suggesting that the analytical approximation for the modes works to a very good accuracy. Notice that, around the bounce, the amplitude of the scalar perturbations are enhanced by a few orders of magnitude more than that of the tensor perturbations. It is this feature, which is obviously a result of the specific behavior of the background near the bounce, that leads to a viable tensor-to-scalar ratio.

the bounce have been evaluated at $\eta = \beta\,\eta_0$, with $\beta = 10^2$, which, recall that, corresponds to $\mathcal{N} = 4.3$. Since the scales of cosmological interest are much smaller than the scale associated with the bounce, the shapes of the power spectra are indeed expected to remain unaffected by the bounce. While a bounce generically enhances the amplitude of the perturbations, the scalar and tensor perturbations can be expected to be amplified by different amounts, depending on the behavior of the background close to the bounce. Note that, in the scenario of our interest, the tensor-to-scalar ratio is rather large before the bounce. In fact, the tensor-to-scalar ratio well before the bounce proves to be of the order of $\mathcal{O}(24)$, a result that is well known in the literature (see, for instance, Ref. [30]). As we had pointed out, in our case, the bounce amplifies the scalar perturbations much more than the tensor perturbations [cf. Figs. 4 and 5]. In other words, the bounce suppresses the tensor-to-scalar ratio. Recall that, the only parameter that occurs in our model is the combination k_0/a_0. We find that, for a choice of k_0/a_0 that leads to a COBE normalized scalar power spectrum after the bounce, *i.e.* $\mathcal{P}_{_\mathcal{R}}(k) \simeq 2.31 \times 10^{-9}$ [85], the corresponding tensor-to-scalar ratio proves to be much smaller than the current upper bound of $r < 0.1$ from Planck [60]. It is also useful to note

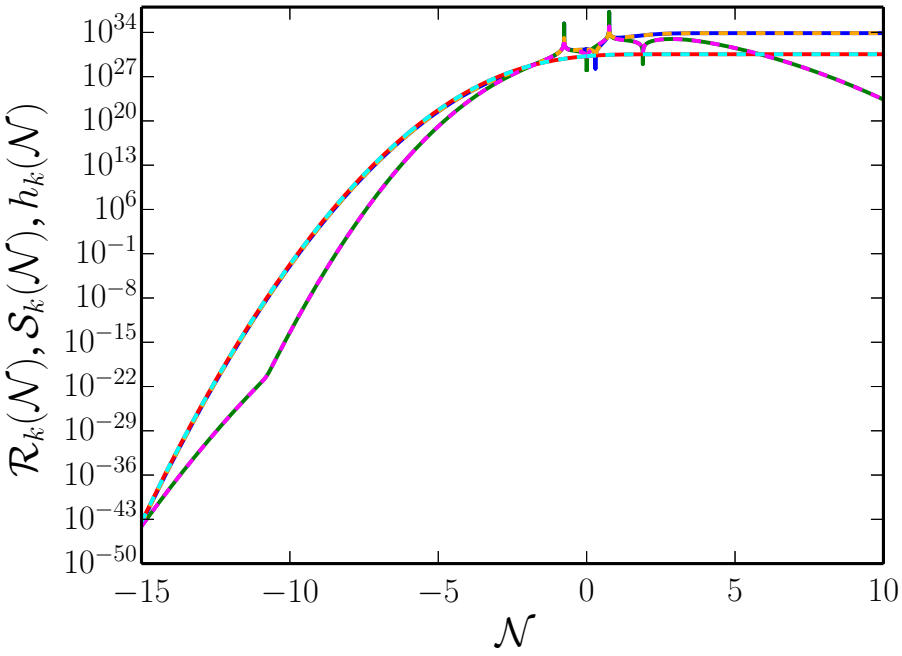

Figure 5. The plots as in the previous figure for the wavenumber $k/k_0 = 10^{-25}$. Clearly, the analytical results are in good agreement with the numerical results.

that isocurvature perturbations, while they grow across the bounce, begin to decay at late times (actually, after $\eta > \eta_*$). At a sufficiently late time when we evaluate the power spectra, their amplitude proves to be about four orders of magnitude smaller than the amplitude of the curvature perturbation. This suggests that the power spectrum is strongly adiabatic, which is also consistent with the recent observations [60].

Let us now evaluate the scalar power spectra analytically after the bounce. At a sufficiently late time after the bounce (say, when $\eta \gg \eta_*$), we find that the curvature perturbation turns almost a constant [cf. Eq. (7.7a)], and is given by

$$\mathcal{R}_k(\eta) \simeq \mathcal{C}_k \, \frac{\pi}{4\, a_0^2} - \mathcal{E}_k \, \frac{\mathrm{e}^{-\sqrt{5}\pi}}{3} - \mathcal{F}_k \, \frac{\mathrm{e}^{\sqrt{5}\,\pi}}{3} + \mathcal{D}_k. \tag{8.1}$$

We have plotted the power spectrum associated with this curvature perturbation in Fig. 7, which is very similar in shape to the analytical tensor power spectrum we had plotted earlier [cf. Fig. 2]. Note that our analytical approximations are valid only when $k \ll k_0/\alpha$, and the spectrum is indeed scale invariant over this domain, reflecting the behavior obtained numerically. If we now assume that $k \ll k_0/\alpha$, we obtain the scale invariant amplitude of the curvature perturbation spectrum to be

$$\mathcal{P}_{\mathcal{R}}(k) \simeq \frac{k_0^2 \, \mathrm{e}^{4\,\sqrt{5}\,\pi}}{61440\, \pi^2\, a_0^2\, M_{_{\mathrm{Pl}}}^2}, \tag{8.2}$$

which we find matches the numerical result [of COBE normalized amplitude for $k_0/(a_0\, M_{_{\mathrm{Pl}}}) = 3.3 \times 10^{-8}$] very well.

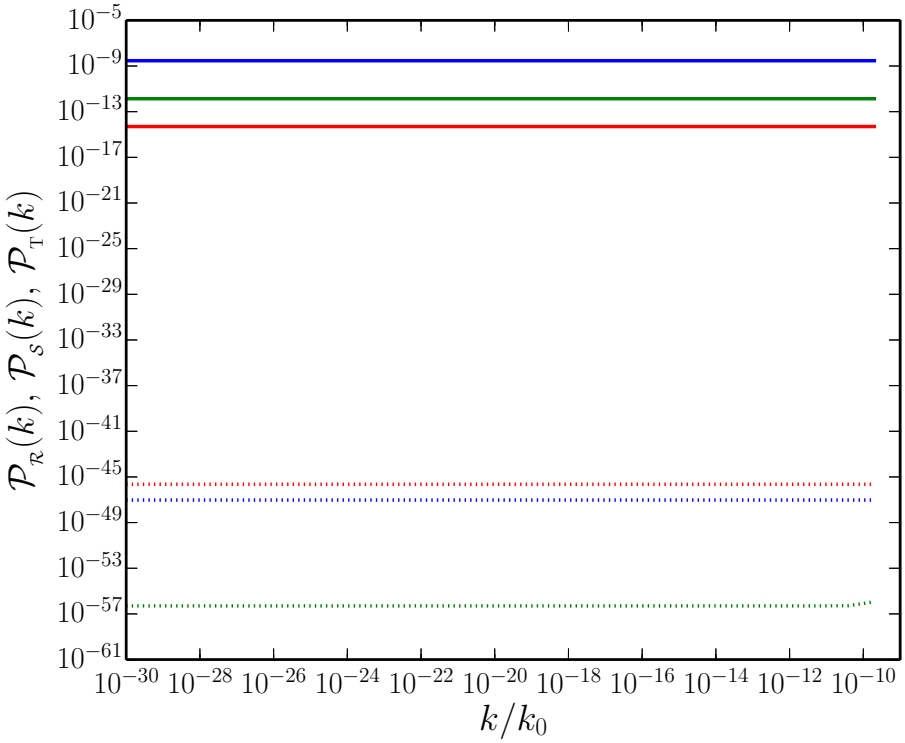

Figure 6. The numerically evaluated scalar (the curvature perturbation spectrum in blue and the isocurvature perturbation spectrum in green) and tensor power spectra (in red) have been plotted as a function of k/k_0 for a wide range of wavenumbers. The power spectra have been plotted both before the bounce (as dotted lines) and after (as solid lines). The power spectra have been evaluated at $\eta = -\alpha\,\eta_0$ (with $\alpha = 10^5$) before the bounce and at $\eta = \beta\,\eta_0$ (with $\beta = 10^2$) after the bounce. In plotting the figure, we have set $k_0/(a_0\,M_{_{\rm Pl}}) = 3.3 \times 10^{-8}$, as in the previous figures. All the power spectra are evidently scale invariant over scales of cosmological interest. Also, the above choice of k_0/a_0 leads to a COBE normalized curvature perturbation spectrum. Moreover, the tensor-to-scalar ratio evaluated after the bounce proves to be rather small ($r \simeq 10^{-6}$), which is consistent with the current upper limits on the quantity.

From the analytical and numerical results for the scalar and tensor modes, we can also understand the behavior of the tensor-to-scalar ratio across the bounce. In Fig. 8, we have plotted the evolution of the tensor-to-scalar $r_k = \mathcal{P}_{_{\rm T}}(k)/\mathcal{P}_{\mathcal{R}}(k)$ for a given mode with wavenumber $k/k_0 = 10^{-20}$. We have plotted the numerical as well as the analytical results in the figure. The numerical and the analytical results agree well with each other. Also, r_k vanishes (at $\eta = \mp\eta_*$) and diverges (during $0 < \eta < \eta_*$) exactly reflecting the behavior of the curvature perturbation (which diverges and vanishes at these points, respectively). Importantly, the bounce suppresses the tensor-to-scalar ratio from a large value ($r_k \simeq 20$) to a rather small value ($r_k \simeq 10^{-6}$) that is consistent with the current upper bounds. It is interesting to note that tensor-to-scalar ratio is a pure number and is actually independent of even the single parameter k_0/a_0 that characterizes our model [cf. Eqs. (3.17) and (8.2)].

Our last task is to arrive at the isocurvature power spectrum analytically. At large times after the bounce (such that $\eta \gg \eta_*$), the behavior of the isocurvature perturbation can

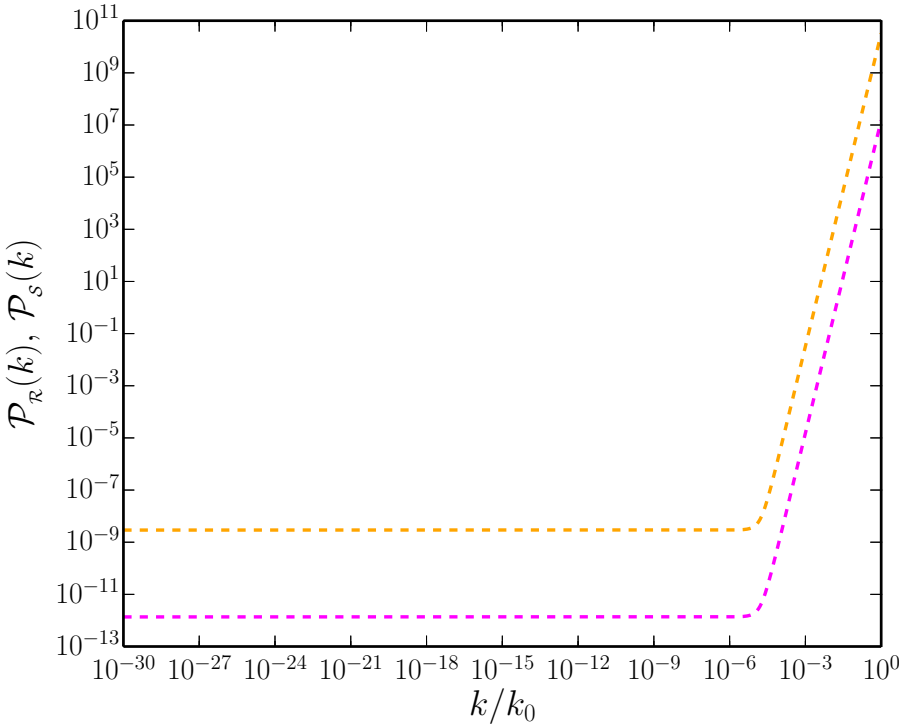

Figure 7. The curvature (in orange) and the isocurvature (in magenta) perturbation spectra evaluated analytically after the bounce. In plotting this figure, we have chosen the same values for the various parameters as in Fig. 2, wherein we had plotted the tensor power spectrum obtained analytically. As in the case of the tensor power spectrum, these analytical spectra are valid only for $k \ll k_0/\alpha$. We find that the scale invariant amplitudes at such small wavenumbers match the numerical results presented in the previous figure very well.

be shown to be [cf. Eq. (7.7b)]

$$\mathcal{S}_k(\eta) \simeq \frac{4\,\mathcal{F}_k\,\mathrm{e}^{\sqrt{5}\,\pi}}{3\,\sqrt{3}\,k_0\,\eta}. \tag{8.3}$$

Unlike the curvature perturbation, the isocurvature perturbation is not a constant in this domain, but decays with the expansion of the universe. This behavior is also evident from the numerical results [cf. Figs. 4 and 5]. For scales of cosmological interest such that $k \ll k_0/\alpha$, we find that the isocurvature perturbation spectrum, evaluated at $\eta = \beta\,\eta_0$, is given by

$$\mathcal{P}_{\mathcal{S}}(k) \simeq \frac{k_0^2\,\mathrm{e}^{4\,\sqrt{5}\,\pi}}{11520\,\beta^2\,\pi^2\,a_0^2\,M_{_{\mathrm{Pl}}}^2}. \tag{8.4}$$

For the values of the parameters we have been working with, *viz.* $k_0/(a_0\,M_{_{\mathrm{Pl}}}) = 3.3 \times 10^{-8}$ and $\beta = 10^2$, we find that the above analytical estimate agrees well with the numerical results we have obtained.

9 Summary and outlook

One of the problems that had plagued completely symmetric bouncing scenarios is the fact that the tensor-to-scalar ratio in such models proves to be large, typically well beyond the

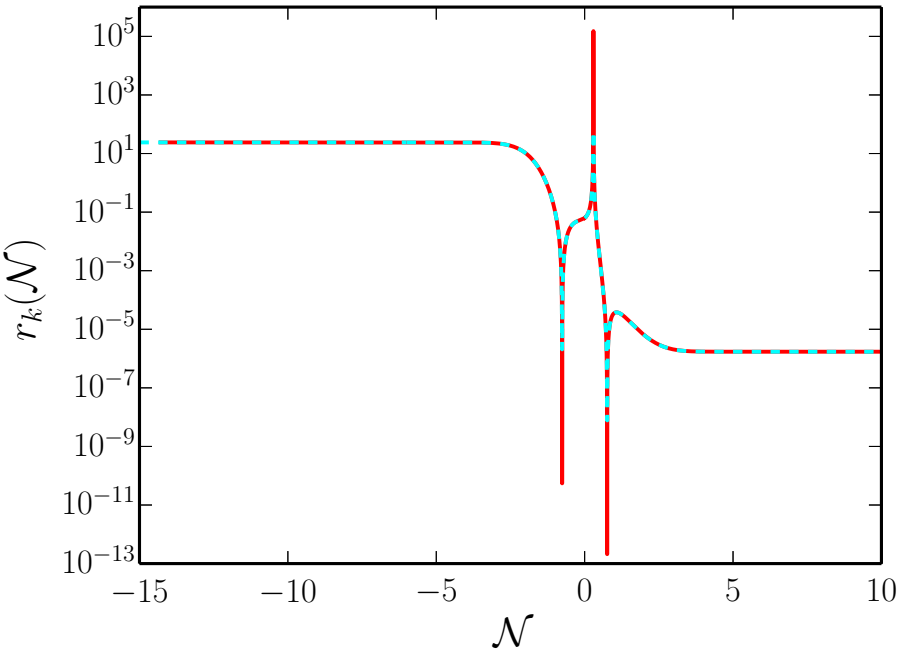

Figure 8. The tensor-to-scalar ratio calculated numerically (red solid line) and analytically (cyan dashed line) have been plotted as a function of $\mathcal{N}$ for the wavenumber $k/k_0 = 10^{-20}$. The numerical and the analytical results agree well as expected. Note that the bounce suppresses the tensor-to-scalar ratio from a large value ($r_k \simeq 20$) to a rather small value ($r_k \simeq 10^{-6}$).

current constraints from the cosmological data. In this work, we have constructed a two field model consisting of a canonical scalar field and a non-canonical ghost field to drive a symmetric matter bounce and have studied the evolution of the scalar and tensor perturbations in the model. For a specific choice of the scale factor describing the matter bounce, we have been able to arrive at completely analytical solutions for all the background quantities. We find that the model we have constructed involves only one parameter, *viz.* the ratio of the scale associated with the bounce to the value of the scale factor at the bounce. Using the background solutions, we have numerically evolved the perturbations across the bounce and have evaluated the scalar and tensor power spectra after the bounce. In order to circumvent the issues confronting the evolution of the curvature and the isocurvature perturbations in a bouncing scenario, we have worked in a specific gauge wherein the two independent scalar perturbations behave well across the bounce. Once having evolved the perturbations, we reconstruct the curvature and the isocurvature perturbations from these quantities and evaluate the corresponding power spectra. We show that the scalar and tensor perturbation spectra in our model prove to be strictly scale invariant, as is expected to occur in a matter bounce scenario. We also explicitly illustrate a well understood result, *viz.* while the bounce affects the amplitudes of the power spectra, their shapes remain unmodified across the bounce over scales of cosmological interest. Moreover, we find that, for a value of the scale factor that leads to the COBE normalized power spectrum for the curvature perturbation, the tensor-to-scalar ratio proves to be of the order of $r \simeq 10^{-6}$, which is, obviously, perfectly consistent with the current upper bounds from the recent CMB observations. Further, we have shown that, the amplitude of the isocurvature perturbations are quite small (their power spectrum

is about four orders of magnitude below the power spectrum of the curvature perturbation). This indicates that the scenario generates a strongly adiabatic scalar perturbation spectra, again an aspect which is consistent with the observations. Importantly, we also support all the numerical results with analytical arguments.

Before, we conclude, we believe we should clarify a few different points. As we have pointed out repeatedly, our model essentially depends on only one parameter, *viz.* k_0/a_0. This is evident from potential governing the model and this aspect is also reflected in the results we have obtained. Notice that the amplitudes of the scalar as well as the tensor power spectra [cf. Eqs. (3.17), (8.2) and (8.4)] actually depend only on the ratio $k_0/(M_{_{\rm Pl}}\, a_0)$. We have chosen $k_0/(a_0\, M_{_{\rm Pl}}) = 3.3 \times 10^{-8}$ in order to lead to a COBE normalized curvature perturbation spectrum. It is also important to note that, in terms of cosmic time, the duration of the bounce is, in fact, of the order of $a_0\, \eta_* \simeq a_0/k_0$.

Another point that requires some clarification is the assumption of a symmetric bounce. The assumption of a symmetric bounce has proved to be convenient for us to study the problem. Actually, the scale factor and the model that drives the background will be valid only until an early epoch after the bounce. Hence, the term symmetric bounce basically refers to the period close to the bounce. At a suitable time after the bounce, we expect the energy from the scalar fields to be transferred to radiation as is done, for instance, in perturbative reheating after inflation. Though we have not touched upon this issue here, we believe that reheating can be achieved with a simple coupling (such as the conventional $\Gamma\, \dot{\phi}$ term) between the scalar field and the radiation fluid. Since we expect reheating to be achieved in such a fashion, we have ignored the presence of a radiation fluid in this work.

While it is interesting to have achieved a tensor-to-scalar ratio that is consistent with the observations in a completely symmetric matter bounce scenario, needless to add, many challenges remain. Theoretically, the model needs to be examined in greater detail to understand the fundamental reason as to why it leads to a small tensor-to-scalar ratio. In this context, the best way forward seems to be to consider different models leading to the same factor and investigate the behavior of the perturbations in these different models. Another related point is regarding the concern that has been raised about the situations under which the standard initial conditions can be imposed (in this context, see, for instance, Ref. [82]). In the case of our model, since the curvature and the isocurvature perturbations decouple during the early contracting phase, we have been able to impose the standard Bunch-Davies initial conditions.

From an observational point of view, we need to generate a tilt in the scalar power spectrum to match the CMB observations. Moreover, we need to examine if the scalar non-Gaussianities generated in the model are indeed consistent with the current constraints from Planck [88]. Further, rather than brush them aside, we need to get around to addressing the different theoretical issues plaguing bouncing models that we had discussed in some detail in the introductory section. We should point out here that a completely nonperturbative analysis of a model very similar to what we have considered seems to suggest such models may not be as pathological as it has been argued to be [89]. Clearly, one needs to explore more complex models beyond the simple model we have constructed here. We are presently investigating a variety of such issues.

Acknowledgements

DC would like to thank the Indian Institute of Technology Madras, Chennai, India, for financial support through half-time research assistantship. LS wishes to thank Rishi Khatri for discussions. The authors thank Robert Brandenberger, Patrick Peter and V. Sreenath for comments on the manuscript.

A Fixing the coefficients

Recall that, in Sec. 7, the expressions (7.7a) and (7.7b) that describe the analytical solutions for $\mathcal{R}_k$ and $\mathcal{S}_k$ in the second domain had contained four time-independent constants, *viz.* $\mathcal{C}_k$, $\mathcal{D}_k$, $\mathcal{E}_k$ and $\mathcal{F}_k$. As we had described, these four constants are to be determined by matching the solutions for $\mathcal{R}_k$ and $\mathcal{S}_k$ in the first domain [cf. Eqs. (7.1) and (7.2)] and their time derivatives with the corresponding quantities in the second domain. This matching has to be carried out at the junction of the two domains, *viz.* at $\eta = -\alpha\,\eta_0$. These matching conditions lead to four equations which need to be solved simultaneously to arrive at the constants. The constants can be determined to be

$$
\begin{aligned}
\mathcal{C}_k = \frac{\left(\alpha^2+1\right)\,a_0}{54\,\sqrt{2}\,\alpha^7\,k_0^2\,M_{_{\rm Pl}}\,k^{3/2}}\,\Bigg\{ & 16\,\alpha^2\,\sqrt{\alpha^2+1}\,k^2 \\
& \times\,\left[\alpha\,\left(\alpha^2+1\right)\,k - 3\,\sqrt{3}\,i\,\left(\alpha^2-1\right)\,k_0\right]\,\mathrm{Ei}\left[i\,\left(3-\sqrt{3}\right)\,\alpha\,k/(3\,k_0)\right]\,\mathrm{e}^{i\,\alpha\,k/(\sqrt{3}\,k_0)} \\
& + \sqrt{3}\,\Bigg[i\,\alpha^2\,\left(\alpha^2+1\right)\,\left(-9\,\alpha^3+32\,\sqrt{\alpha^2+1}+27\,\alpha\right)\,k_0\,k^2 \\
& + \left(9\,\alpha^5-18\,\alpha^3+16\,\alpha^2\,\sqrt{\alpha^2+1}-80\,\sqrt{\alpha^2+1}-27\,\alpha\right)\,\left(3\,\alpha\,k_0^2\,k+3\,i\,k_0^3\right)\Bigg]\,\mathrm{e}^{i\,\alpha\,k/k_0} \\
& - 4\,\alpha^2\,\sqrt{\alpha^2+1}\,\left(4\,\pi\,k^2+3^{7/4}\,k_0\,k\right)\left[3\,\sqrt{3}\,\left(\alpha^2-1\right)\,k_0+i\,\alpha\,\left(\alpha^2+1\right)\,k\right]\,\mathrm{e}^{i\,\alpha\,k/(\sqrt{3}\,k_0)}\Bigg\},
\end{aligned}
\tag{A.1}
$$

$$
\begin{aligned}
\mathcal{D}_k = \frac{1}{108\sqrt{2}\,3^{3/4}\,\alpha^7\,a_0\,k_0^2\,M_{\rm Pl}\,k^{3/2}} \Bigg\{ & 4\,3^{1/4}\,\alpha^2\,\sqrt{\alpha^2+1}\left(\sqrt{3}\,\alpha^2\,\left(\alpha^2+1\right)\,k^3\right. \\
& \left. -9\,i\,\alpha\,\left(4\,\alpha^2-1\right)\,k_0\,k^2+\left[4\sqrt{3}\,\alpha\,\left(\alpha^2+1\right)^2\,k-36\,i\,\left(\alpha^4-1\right)\,k_0\right]\,k^2\,\tan^{-1}(\alpha)\right) \\
& \times \mathrm{Ei}\left[i\,\left(3-\sqrt{3}\right)\,\alpha\,k/(3\,k_0)\right]\,\mathrm{e}^{i\,\alpha\,k/(\sqrt{3}\,k_0)} \\
& +3^{5/4}\,\alpha\left[i\,\alpha^2\,\left(\alpha^2+1\right)\,\left(-9\,\alpha^3+8\,\sqrt{\alpha^2+1}+9\,\alpha\right)\,k_0\,k^2\right. \\
& \left.+\left(9\,\alpha^5+12\,\alpha^3+40\,\alpha^2\,\sqrt{\alpha^2+1}-20\,\sqrt{\alpha^2+1}-9\,\alpha\right)\,\left(3\,\alpha\,k_0^2\,k+3\,i\,k_0^3\right)\right]\mathrm{e}^{i\,\alpha\,k/k_0} \\
& +\alpha^2\,\sqrt{\alpha^2+1}\,\left(4\,3^{1/4}\,\pi\,k^2+9\,k_0\,k\right)\,\left[\left(9-36\,\alpha^2\right)\,k_0-i\,\sqrt{3}\,\alpha\,\left(\alpha^2+1\right)\,k\right]\mathrm{e}^{i\,\alpha\,k/(\sqrt{3}\,k_0)} \\
& +\left(\alpha^2+1\right)\,\tan^{-1}(\alpha)\left[3^{5/4}\,i\,\alpha^2\,\left(\alpha^2+1\right)\,\left(-9\,\alpha^3+32\,\sqrt{\alpha^2+1}+27\,\alpha\right)\,k_0\,k^2\right. \\
& \left.+3^{9/4}\,\left(9\,\alpha^5-18\,\alpha^3+16\,\sqrt{\alpha^2+1}\,\alpha^2-80\,\sqrt{\alpha^2+1}-27\,\alpha\right)\,\left(\alpha\,k_0^2\,k+i\,k_0^3\right)\right]\mathrm{e}^{i\,\alpha\,k/k_0} \\
& +4\,\alpha^2\,\left(\alpha^2+1\right)^{3/2}\,\tan^{-1}(\alpha)\,\left(4\,3^{1/4}\,\pi\,k+9\,k_0\right) \\
& \times\left[-9\,\left(\alpha^2-1\right)\,k_0\,k-\sqrt{3}\,i\,\alpha\,\left(\alpha^2+1\right)\,k^2\right]\mathrm{e}^{i\,\alpha\,k/(\sqrt{3}\,k_0)}\Bigg\}, \qquad \text{(A.2)}
\end{aligned}
$$

$$
\begin{aligned}
\mathcal{E}_k = & \frac{\mathrm{e}^{-2\sqrt{5}\,\tan^{-1}(\alpha)}}{864\;3^{3/4}\,\sqrt{10}\,\alpha^7\;\left(\alpha+\sqrt{5}\right)\;a_0\,k_0^2\,M_{\rm Pl}\,k^{3/2}}\Bigg\{-16\;3^{1/4}\,\alpha^2\,\sqrt{\alpha^2+1}\,k^2\;\mathrm{e}^{i\,\alpha\,k/(\sqrt{3}\,k_0)} \\
& \times\left[\sqrt{3}\,\alpha\left(\alpha^2+1\right)\;\left(4\,\alpha^3+5\,\sqrt{5}\,\alpha^2+8\,\alpha+3\,\sqrt{5}\right)\;k+9\,i\;\left(\sqrt{5}\,\alpha^2+8\,\alpha+3\,\sqrt{5}\right)\;k_0\right] \\
& \times\mathrm{Ei}\left[i\;\left(3-\sqrt{3}\right)\;\alpha\,k/(3\,k_0)\right] \\
& +\Bigg(-i\,\alpha^2\;\left(\alpha^2+1\right)\;\Big[-9\,\alpha^6+9\,\sqrt{5}\,\alpha^5+162\,\alpha^4+\left(160\,\sqrt{5\,(\alpha^2+1)}+171\right)\alpha^2 \\
& +\left(256\,\sqrt{\alpha^2+1}+81\,\sqrt{5}\right)\;\alpha+96\,\sqrt{5\,(\alpha^2+1)}+2\;\left(64\,\sqrt{\alpha^2+1}+45\,\sqrt{5}\right)\;\alpha^3\Big]\;k^2 \\
& +\Big[-9\,\alpha^8+9\,\sqrt{5}\,\alpha^7+153\,\alpha^6+19\;\left(16\,\sqrt{5\,(\alpha^2+1)}+9\right)\;\alpha^2 \\
& +\left(640\,\sqrt{\alpha^2+1}+81\,\sqrt{5}\right)\;\alpha+240\,\sqrt{5\,(\alpha^2+1)}+\left(128\,\sqrt{\alpha^2+1}+99\,\sqrt{5}\right)\;\alpha^5 \\
& +\left(160\,\sqrt{5\,(\alpha^2+1)}+333\right)\alpha^4+3\;\left(128\,\sqrt{\alpha^2+1}+57\,\sqrt{5}\right)\;\alpha^3\Big]\;\left(3\,\alpha\,k_0\,k+3\,i\,k_0^2\right)\Bigg) \\
& \times 3^{5/4}\,k_0\,\mathrm{e}^{i\,\alpha\,k/k_0} \\
& +4\,i\,\alpha^2\,\sqrt{\alpha^2+1}\;\left(4\,3^{1/4}\,\pi\,k^2+9\,k_0\,k\right)\;\Big[9\,i\;\left(\sqrt{5}\,\alpha^2+8\,\alpha+3\,\sqrt{5}\right)\;k_0 \\
& +\sqrt{3}\,\alpha\;\left(\alpha^2+1\right)\;\left(4\,\alpha^3+5\,\sqrt{5}\,\alpha^2+8\,\alpha+3\,\sqrt{5}\right)\;k\Big]\;\mathrm{e}^{i\,\alpha\,k/(\sqrt{3}\,k_0)}\Bigg\},
\end{aligned}
\tag{A.3}
$$

$$
\begin{aligned}
\mathcal{F}_k = & \frac{\mathrm{e}^{2\sqrt{5}\,\tan^{-1}(\alpha)}}{864\,3^{3/4}\sqrt{10}\,\alpha^7\,\left(\alpha+\sqrt{5}\right)\,a_0\,k_0^2\,M_{\rm Pl}\,k^{3/2}}\Bigg\{16\,3^{1/4}\,\alpha^2\,\sqrt{\alpha^2+1}\,k^2 \\
& \times\left[\sqrt{3}\,\alpha\,\left(\alpha^2+1\right)\,\left(4\,\alpha^3+3\,\sqrt{5}\,\alpha^2-2\,\alpha+3\,\sqrt{5}\right)\,k-9\,i\,\left(\sqrt{5}\,\alpha^2+2\,\alpha-3\,\sqrt{5}\right)\,k_0\right] \\
& \times\mathrm{Ei}\left[i\,\left(3-\sqrt{3}\right)\,\alpha\,k/(3\,k_0)\right]\,\mathrm{e}^{i\,\alpha\,k/(\sqrt{3}\,k_0)} \\
& +\Bigg(i\,\alpha^2\,\left(\alpha^2+1\right)\,\Bigg[-9\,\alpha^6-27\,\sqrt{5}\,\alpha^5-18\,\alpha^4+\left(96\,\sqrt{5\,(\alpha^2+1)}-9\right)\,\alpha^2 \\
& +\left(81\,\sqrt{5}-64\,\sqrt{\alpha^2+1}\right)\,\alpha+96\,\sqrt{5\,(\alpha^2+1)}+2\,\left(64\,\sqrt{\alpha^2+1}+27\,\sqrt{5}\right)\,\alpha^3\Bigg]k^2 \\
& -\Bigg[-9\,\alpha^8-27\,\sqrt{5}\,\alpha^7-27\,\alpha^6+9\,\left(16\,\sqrt{5\,(\alpha^2+1)}-1\right)\,\alpha^2 \\
& +\left(81\,\sqrt{5}-160\,\sqrt{\alpha^2+1}\right)\,\alpha+240\,\sqrt{5\,(\alpha^2+1)}+\left(128\,\sqrt{\alpha^2+1}+27\,\sqrt{5}\right)\,\alpha^5 \\
& +3\,\left(32\,\sqrt{5\,(\alpha^2+1)}-9\right)\,\alpha^4+\left(64\,\sqrt{\alpha^2+1}+135\,\sqrt{5}\right)\,\alpha^3\Bigg]\,\left(3\,\alpha\,k_0\,k+3\,i\,k_0^2\right)\Bigg) \\
& \times 3^{5/4}\,k_0\,\mathrm{e}^{i\,\alpha\,k/k_0} \\
& -4\,\alpha^2\,\sqrt{\alpha^2+1}\,\left(4\,3^{1/4}\,\pi\,k^2+9\,k_0\,k\right)\,\Bigg[9\,\left(\sqrt{5}\,\alpha^2+2\,\alpha-3\,\sqrt{5}\right)\,k_0 \\
& +\sqrt{3}\,i\,\alpha\,\left(\alpha^2+1\right)\,\left(4\,\alpha^3+3\,\sqrt{5}\,\alpha^2-2\,\alpha+3\,\sqrt{5}\right)\,k\Bigg]\,\mathrm{e}^{i\,\alpha\,k/(\sqrt{3}\,k_0)}\Bigg\}. \qquad \text{(A.4)}
\end{aligned}
$$

References

[1] M. Novello and S. P. Bergliaffa, *Bouncing Cosmologies*, *Phys.Rept.* **463** (2008) 127–213, [arXiv:0802.1634].

[2] Y.-F. Cai, *Exploring Bouncing Cosmologies with Cosmological Surveys*, *Sci. China Phys. Mech. Astron.* **57** (2014) 1414–1430, [arXiv:1405.1369].

[3] D. Battefeld and P. Peter, *A Critical Review of Classical Bouncing Cosmologies*, *Phys.Rept.* **571** (2015) 1–66, [arXiv:1406.2790].

[4] M. Lilley and P. Peter, *Bouncing alternatives to inflation*, *Comptes Rendus Physique* **16** (2015) 1038–1047, [arXiv:1503.06578].

[5] A. Ijjas and P. J. Steinhardt, *Implications of Planck2015 for inflationary, ekpyrotic and anamorphic bouncing cosmologies*, *Class. Quant. Grav.* **33** (2016), no. 4 044001, [arXiv:1512.09010].

[6] R. Brandenberger and P. Peter, *Bouncing Cosmologies: Progress and Problems*, arXiv:1603.05834.

[7] V. F. Mukhanov, H. A. Feldman, and R. H. Brandenberger, *Theory of cosmological perturbations*, *Physics Reports* **215** (1992), no. 5 203–333.

[8] J. Martin, *Inflation and precision cosmology*, *Braz. J. Phys.* **34** (2004) 1307–1321, [astro-ph/0312492].

[9] J. Martin, *Inflationary cosmological perturbations of quantum-mechanical origin*, *Lect. Notes Phys.* **669** (2005) 199–244, [hep-th/0406011]. [,199(2004)].

[10] B. A. Bassett, S. Tsujikawa, and D. Wands, *Inflation dynamics and reheating*, *Rev. Mod. Phys.* **78** (May, 2006) 537–589.

[11] L. Sriramkumar, *An introduction to inflation and cosmological perturbation theory*, arXiv:0904.4584.

[12] L. Sriramkumar, *On the generation and evolution of perturbations during inflation and reheating*, in *Vignettes in Gravitation and Cosmology* (L. Sriramkumar and T. Seshadri, eds.), pp. 207–249. World Scientific, Singapore, 2012.

[13] D. Baumann, *Inflation*, in *Physics of the large and the small, TASI 09, proceedings of the Theoretical Advanced Study Institute in Elementary Particle Physics, Boulder, Colorado, USA, 1-26 June 2009*, pp. 523–686, 2011. arXiv:0907.5424.

[14] A. Linde, *Inflationary Cosmology after Planck 2013*, in *Proceedings, 100th Les Houches Summer School: Post-Planck Cosmology: Les Houches, France, July 8 - August 2, 2013*, pp. 231–316, 2015. arXiv:1402.0526.

[15] J. Martin, *The Observational Status of Cosmic Inflation after Planck*, *Astrophys. Space Sci. Proc.* **45** (2016) 41–134, [arXiv:1502.05733].

[16] J. Martin, C. Ringeval, and R. Trotta, *Hunting Down the Best Model of Inflation with Bayesian Evidence*, *Phys. Rev.* **D83** (2011) 063524, [arXiv:1009.4157].

[17] J. Martin, C. Ringeval, and V. Vennin, *Encyclopædia Inflationaris*, *Phys.Dark Univ.* **5-6** (2014) 75–235, [arXiv:1303.3787].

[18] J. Martin, C. Ringeval, R. Trotta, and V. Vennin, *The Best Inflationary Models After Planck*, *JCAP* **1403** (2014) 039, [arXiv:1312.3529].

[19] J. Martin, C. Ringeval, and V. Vennin, *How Well Can Future CMB Missions Constrain Cosmic Inflation?*, *JCAP* **1410** (2014), no. 10 038, [arXiv:1407.4034].

[20] G. Gubitosi, M. Lagos, J. Magueijo, and R. Allison, *Bayesian evidence and predictivity of the inflationary paradigm*, *JCAP* **1606** (2016), no. 06 002, [arXiv:1506.09143].

[21] S. D. P. Vitenti and N. Pinto-Neto, *Large Adiabatic Scalar Perturbations in a Regular Bouncing Universe*, *Phys. Rev.* **D85** (2012) 023524, [arXiv:1111.0888].

[22] N. Pinto-Neto and S. D. P. Vitenti, *Comment on "Growth of covariant perturbations in the contracting phase of a bouncing universe"*, *Phys. Rev.* **D89** (2014), no. 2 028301, [arXiv:1312.7790].

[23] D. A. Easson and A. Vikman, *The Phantom of the New Oscillatory Cosmological Phase*, arXiv:1607.00996.

[24] V. A. Belinsky, I. M. Khalatnikov, and E. M. Lifshitz, *Oscillatory approach to a singular point in the relativistic cosmology*, *Adv. Phys.* **19** (1970) 525–573.

[25] J. Khoury, B. A. Ovrut, P. J. Steinhardt, and N. Turok, *The Ekpyrotic universe: Colliding branes and the origin of the hot big bang*, *Phys. Rev.* **D64** (2001) 123522, [hep-th/0103239].

[26] J. Khoury, B. A. Ovrut, P. J. Steinhardt, and N. Turok, *Density perturbations in the ekpyrotic scenario*, *Phys. Rev.* **D66** (2002) 046005, [hep-th/0109050].

[27] J.-L. Lehners, *Ekpyrotic and Cyclic Cosmology*, *Phys. Rept.* **465** (2008) 223–263, [arXiv:0806.1245].

[28] A. M. Levy, A. Ijjas, and P. J. Steinhardt, *Scale-invariant perturbations in ekpyrotic cosmologies without fine-tuning of initial conditions*, *Phys. Rev.* **D92** (2015), no. 6 063524, [arXiv:1506.01011].

[29] A. M. Levy, *Fine-tuning challenges for the matter bounce scenario*, arXiv:1611.08972.

[30] L. E. Allen and D. Wands, *Cosmological perturbations through a simple bounce*, *Phys. Rev.*

D70 (2004) 063515, [astro-ph/0404441].

[31] T. J. Battefeld and R. Brandenberger, *Vector perturbations in a contracting universe*, *Phys. Rev.* **D70** (2004) 121302, [hep-th/0406180].

[32] J. Martin, P. Peter, N. Pinto Neto, and D. J. Schwarz, *Passing through the bounce in the ekpyrotic models*, *Phys.Rev.* **D65** (2002) 123513, [hep-th/0112128].

[33] S. Tsujikawa, R. Brandenberger, and F. Finelli, *On the construction of nonsingular pre - big bang and ekpyrotic cosmologies and the resulting density perturbations*, *Phys.Rev.* **D66** (2002) 083513, [hep-th/0207228].

[34] P. Peter and N. Pinto-Neto, *Primordial perturbations in a non singular bouncing universe model*, *Phys. Rev.* **D66** (2002) 063509, [hep-th/0203013].

[35] P. Peter, N. Pinto-Neto, and D. A. Gonzalez, *Adiabatic and entropy perturbations propagation in a bouncing universe*, *JCAP* **0312** (2003) 003, [hep-th/0306005].

[36] J. Martin and P. Peter, *Parametric amplification of metric fluctuations through a bouncing phase*, *Phys. Rev.* **D68** (2003) 103517, [hep-th/0307077].

[37] V. Bozza and G. Veneziano, *Scalar perturbations in regular two-component bouncing cosmologies*, *Phys. Lett.* **B625** (2005) 177–183, [hep-th/0502047].

[38] Y.-F. Cai, T. Qiu, Y.-S. Piao, M. Li, and X. Zhang, *Bouncing universe with quintom matter*, *JHEP* **10** (2007) 071, [arXiv:0704.1090].

[39] F. Finelli, P. Peter, and N. Pinto-Neto, *Spectra of primordial fluctuations in two-perfect-fluid regular bounces*, *Phys. Rev.* **D77** (2008) 103508, [arXiv:0709.3074].

[40] Y.-F. Cai, T. Qiu, R. Brandenberger, Y.-S. Piao, and X. Zhang, *On Perturbations of Quintom Bounce*, *JCAP* **0803** (2008) 013, [arXiv:0711.2187].

[41] F. T. Falciano, M. Lilley, and P. Peter, *A Classical bounce: Constraints and consequences*, *Phys. Rev.* **D77** (2008) 083513, [arXiv:0802.1196].

[42] Y.-F. Cai, T.-t. Qiu, R. Brandenberger, and X.-m. Zhang, *A Nonsingular Cosmology with a Scale-Invariant Spectrum of Cosmological Perturbations from Lee-Wick Theory*, *Phys. Rev.* **D80** (2009) 023511, [arXiv:0810.4677].

[43] C. Lin, R. H. Brandenberger, and L. Perreault Levasseur, *A Matter Bounce By Means of Ghost Condensation*, *JCAP* **1104** (2011) 019, [arXiv:1007.2654].

[44] D. A. Easson, I. Sawicki, and A. Vikman, *G-Bounce*, *JCAP* **1111** (2011) 021, [arXiv:1109.1047].

[45] Y.-F. Cai, R. Brandenberger, and X. Zhang, *The Matter Bounce Curvaton Scenario*, *JCAP* **1103** (2011) 003, [arXiv:1101.0822].

[46] T. Qiu, J. Evslin, Y.-F. Cai, M. Li, and X. Zhang, *Bouncing Galileon Cosmologies*, *JCAP* **1110** (2011) 036, [arXiv:1108.0593].

[47] Y.-F. Cai, D. A. Easson, and R. Brandenberger, *Towards a Nonsingular Bouncing Cosmology*, *JCAP* **1208** (2012) 020, [arXiv:1206.2382].

[48] Y.-F. Cai, E. McDonough, F. Duplessis, and R. H. Brandenberger, *Two Field Matter Bounce Cosmology*, *JCAP* **1310** (2013) 024, [arXiv:1305.5259].

[49] Y.-F. Cai, R. Brandenberger, and P. Peter, *Anisotropy in a Nonsingular Bounce*, *Class. Quant. Grav.* **30** (2013) 075019, [arXiv:1301.4703].

[50] Y.-F. Cai, J. Quintin, E. N. Saridakis, and E. Wilson-Ewing, *Nonsingular bouncing cosmologies in light of BICEP2*, *JCAP* **1407** (2014) 033, [arXiv:1404.4364].

[51] S. D. Odintsov and V. K. Oikonomou, *Matter Bounce Loop Quantum Cosmology from $F(R)$*

Gravity, *Phys. Rev.* **D90** (2014), no. 12 124083, [arXiv:1410.8183].

[52] X. Gao, M. Lilley, and P. Peter, *Non-Gaussianity excess problem in classical bouncing cosmologies*, *Phys. Rev.* **D91** (2015), no. 2 023516, [arXiv:1406.4119].

[53] J. Quintin, Z. Sherkatghanad, Y.-F. Cai, and R. H. Brandenberger, *Evolution of cosmological perturbations and the production of non-Gaussianities through a nonsingular bounce: Indications for a no-go theorem in single field matter bounce cosmologies*, *Phys. Rev.* **D92** (2015), no. 6 063532, [arXiv:1508.04141].

[54] S. Nojiri, S. D. Odintsov, and V. K. Oikonomou, *Bounce universe history from unimodular $F(R)$ gravity*, *Phys. Rev.* **D93** (2016), no. 8 084050, [arXiv:1601.04112].

[55] J. Quintin and R. H. Brandenberger, *Black hole formation in a contracting universe*, *JCAP* **1611** (2016), no. 11 029, [arXiv:1609.02556].

[56] A. Ijjas and P. J. Steinhardt, *Classically stable nonsingular cosmological bounces*, *Phys. Rev. Lett.* **117** (2016), no. 12 121304, [arXiv:1606.08880].

[57] A. Fertig, J.-L. Lehners, E. Mallwitz, and E. Wilson-Ewing, *Converting entropy to curvature perturbations after a cosmic bounce*, *JCAP* **1610** (2016), no. 10 005, [arXiv:1607.05663].

[58] D. Wands, *Duality invariance of cosmological perturbation spectra*, *Phys. Rev.* **D60** (1999) 023507, [gr-qc/9809062].

[59] D. Wands, *Cosmological perturbations through the big bang*, *Adv. Sci. Lett.* **2** (2009) 194–204, [arXiv:0809.4556].

[60] **Planck** Collaboration, P. A. R. Ade et al., *Planck 2015 results. XX. Constraints on inflation*, arXiv:1502.02114.

[61] F. T. Falciano, N. Pinto-Neto, and E. S. Santini, *An Inflationary Non-singular Quantum Cosmological Model*, *Phys. Rev.* **D76** (2007) 083521, [arXiv:0707.1088].

[62] P. Peter and N. Pinto-Neto, *Cosmology without inflation*, *Phys. Rev.* **D78** (2008) 063506, [arXiv:0809.2022].

[63] J. M. Cline, S. Jeon, and G. D. Moore, *The Phantom menaced: Constraints on low-energy effective ghosts*, *Phys. Rev.* **D70** (2004) 043543, [hep-ph/0311312].

[64] N. Arkani-Hamed, H.-C. Cheng, M. A. Luty, and S. Mukohyama, *Ghost condensation and a consistent infrared modification of gravity*, *JHEP* **05** (2004) 074, [hep-th/0312099].

[65] D. Chowdhury, V. Sreenath, and L. Sriramkumar, *The tensor bi-spectrum in a matter bounce*, *JCAP* **1511** (2015) 002, [arXiv:1506.06475].

[66] L. Sriramkumar, K. Atmjeet, and R. K. Jain, *Generation of scale invariant magnetic fields in bouncing universes*, *JCAP* **09** (2015) 010, [arXiv:1504.06853].

[67] D. Chowdhury, L. Sriramkumar, and R. K. Jain, *Duality and scale invariant magnetic fields from bouncing universes*, *Phys. Rev.* **D94** (2016), no. 8 083512, [arXiv:1604.02143].

[68] T. S. Bunch and P. C. W. Davies, *Quantum Field Theory in de Sitter Space: Renormalization by Point Splitting*, *Proc. Roy. Soc. Lond.* **A360** (1978) 117–134.

[69] A. A. Starobinsky, *Spectrum of relict gravitational radiation and the early state of the universe*, *JETP Lett.* **30** (1979) 682–685. [Pisma Zh. Eksp. Teor. Fiz.30,719(1979)].

[70] F. Finelli and R. Brandenberger, *On the generation of a scale invariant spectrum of adiabatic fluctuations in cosmological models with a contracting phase*, *Phys. Rev.* **D65** (2002) 103522, [hep-th/0112249].

[71] J. Garriga and V. F. Mukhanov, *Perturbations in k-inflation*, *Phys. Lett.* **B458** (1999) 219–225, [hep-th/9904176].

[72] R. Akhoury, C. S. Gauthier, and A. Vikman, *Stationary Configurations Imply Shift Symmetry: No Bondi Accretion for Quintessence / k-Essence*, *JHEP* **03** (2009) 082, [arXiv:0811.1620].

[73] S. Unnikrishnan and L. Sriramkumar, *A note on perfect scalar fields*, *Phys. Rev.* **D81** (2010) 103511, [arXiv:1002.0820].

[74] O. Pujolas, I. Sawicki, and A. Vikman, *The Imperfect Fluid behind Kinetic Gravity Braiding*, *JHEP* **11** (2011) 156, [arXiv:1103.5360].

[75] F. Arroja and M. Sasaki, *Note on the equivalence of a barotropic perfect fluid with a k-essence scalar field*, *Phys. Rev. D* **81** (May, 2010) 107301.

[76] K. A. Malik and D. Wands, *Adiabatic and entropy perturbations with interacting fluids and fields*, *JCAP* **0502** (2005) 007, [astro-ph/0411703].

[77] K. A. Malik and D. Wands, *Cosmological perturbations*, *Phys. Rept.* **475** (2009) 1–51, [arXiv:0809.4944].

[78] C. Gordon, D. Wands, B. A. Bassett, and R. Maartens, *Adiabatic and entropy perturbations from inflation*, *Phys. Rev.* **D63** (2001) 023506, [astro-ph/0009131].

[79] D. Langlois and S. Renaux-Petel, *Perturbations in generalized multi-field inflation*, *JCAP* **0804** (2008) 017, [arXiv:0801.1085].

[80] D. Langlois, S. Renaux-Petel, D. A. Steer, and T. Tanaka, *Primordial perturbations and non-Gaussianities in DBI and general multi-field inflation*, *Phys. Rev.* **D78** (2008) 063523, [arXiv:0806.0336].

[81] T. Battefeld, S. P. Patil, and R. Brandenberger, *Non-singular perturbations in a bouncing brane model*, *Phys.Rev.* **D70** (2004) 066006, [hep-th/0401010].

[82] P. Peter, N. Pinto-Neto, and S. D. P. Vitenti, *Quantum Cosmological Perturbations of Multiple Fluids*, *Phys. Rev.* **D93** (2016), no. 2 023520, [arXiv:1510.06628].

[83] S. Tsujikawa, D. Parkinson, and B. A. Bassett, *Correlation - consistency cartography of the double inflation landscape*, *Phys. Rev.* **D67** (2003) 083516, [astro-ph/0210322].

[84] Z. Lalak, D. Langlois, S. Pokorski, and K. Turzynski, *Curvature and isocurvature perturbations in two-field inflation*, *JCAP* **0707** (2007) 014, [arXiv:0704.0212].

[85] E. F. Bunn, A. R. Liddle, and M. J. White, *Four-year COBE normalization of inflationary cosmologies*, *Phys. Rev.* **D54** (1996), no. 10 R5917, [astro-ph/9607038].

[86] I. Wolfram Research, "Mathematica."

[87] I. S. Gradshteyn and I. M. Ryzhik, *Table of Integrals, Series, and Products*. Academic Press, New York, 7th ed., 2007.

[88] **Planck** Collaboration, P. A. R. Ade et al., *Planck 2015 results. XVII. Constraints on primordial non-Gaussianity*, arXiv:1502.01592.

[89] B. Xue, D. Garfinkle, F. Pretorius, and P. J. Steinhardt, *Nonperturbative analysis of the evolution of cosmological perturbations through a nonsingular bounce*, *Phys. Rev.* **D88** (2013) 083509, [arXiv:1308.3044].